Conversion of a μ_3-Alkylidyne into a μ_3-Acyl Group at a Trimetal Centre; *X*-Ray Crystal Structures of the Phosphido Bridged Complexes $[WFe_2(\mu_3\text{-}CR)(\mu\text{-}H)(\mu\text{-}PEt_2)(CO)_6(PEt_2H)(\eta\text{-}C_5H_5)]\cdot Et_2O$, $[WFe_2(\mu_3\text{-}CR)(\mu\text{-}PPh_2)_2(CO)_6(\eta\text{-}C_5H_5)]\cdot 0.5\ CH_2Cl_2$, $[WFe_2(\mu_3\text{-}OCCH_2R)(\mu\text{-}PPh_2)_2(CO)_5(\eta\text{-}C_5H_5)]$, and $[WFe_2(\mu\text{-}OCCH_2R)(\mu\text{-}PPh_2)_2(CO)_6(PPh_2H)(\eta\text{-}C_5H_5)]\cdot CH_2Cl_2$ ($R = C_6H_4Me\text{-}4$)†

John C. Jeffery* and Julian G. Lawrence-Smith
Department of Inorganic Chemistry, The University, Bristol BS8 1TS

In diethyl ether at room temperature the complex $[WFe_2(\mu_3\text{-}CR)(\mu\text{-}CO)(CO)_8(\eta\text{-}C_5H_5)]$ (**1**) ($R = C_6H_4Me\text{-}4$) reacts with 1 equivalent of PMe_2Ph or PEt_2H affording the compounds $[WFe_2(\mu_3\text{-}CR)(\mu\text{-}CO)(CO)_7(PR'_3)(\eta\text{-}C_5H_5)]$ [$PR'_3 = PMe_2Ph$ (**2**) or PEt_2H (**3**)]. At ambient temperature solutions of (**3**) slowly (1—2d) lose CO giving the μ-PEt_2 complex $[WFe_2(\mu_3\text{-}CR)(\mu\text{-}H)(\mu\text{-}PEt_2)(CO)_7(\eta\text{-}C_5H_5)]$ (**4**), which exists as a mixture of isomers in which the hydride ligand bridges either a W–Fe (**4a**) or an Fe–Fe (**4b**) bond. In solution (**4a**) and (**4b**) interconvert slowly on the n.m.r. time-scale. The reaction between (**1**) and an excess of PEt_2H gave $[WFe_2(\mu_3\text{-}CR)(\mu\text{-}H)(\mu\text{-}PEt_2)(CO)_6(PEt_2H)(\eta\text{-}C_5H_5)]\cdot Et_2O$ (**5**). The structure of (**5**) was established by a single-crystal *X*-ray diffraction study and consists of a WFe_2 triangle of metal atoms capped by a μ_3-CR ligand [W–Fe(1) 2.763(1), W–Fe(2) 2.830(1), Fe(1)–Fe(2) 2.687(2), W–μ-C 2.042(8), Fe(1)–μ-C 1.960(8), and Fe(2)–μ-C 2.104(8) Å]. One W–Fe bond is bridged by a μ-PEt_2 group and the Fe–Fe bond is bridged by an hydride ligand. The tungsten atom carries a CO and C_5H_5 group. One iron atom is ligated by two CO groups and a terminal PEt_2H ligand which is *trans* to the μ-PEt_2 group, the remaining iron atom carries three approximately orthogonal CO ligands. Thermolysis of (**5**) results in loss of H_2 and formation of the compound $[WFe_2(\mu_3\text{-}CR)(\mu\text{-}PEt_2)_2(CO)_6(\eta\text{-}C_5H_5)]$ (**6**). The conversion of (**5**) into (**6**) may be more readily achieved at room temperature by the addition of a catalytic amount of $Li[BEt_3H]$. The related reaction of complex (**1**) with 1 equivalent of PPh_2H gave $[WFe_2(\mu_3\text{-}CR)(\mu\text{-}H)(\mu\text{-}PPh_2)(CO)_7(\eta\text{-}C_5H_5)]$ (**7**), which has the same structure as the μ-PEt_2 isomer (**4a**). Treatment of (**1**) with an excess of PPh_2H afforded a chromatographically separable mixture of the cluster compounds $[WFe_2(\mu_3\text{-}CR)(\mu\text{-}PPh_2)_2(CO)_6(\eta\text{-}C_5H_5)]\cdot 0.5CH_2Cl_2$ (**8**), $[WFe_2(\mu_3\text{-}OCCH_2R)(\mu\text{-}PPh_2)_2(CO)_5(\eta\text{-}C_5H_5)]$ (**9**), and $[WFe_2(\mu\text{-}OCCH_2R)(\mu\text{-}PPh_2)(CO)_6(PPh_2H)(\eta\text{-}C_5H_5)]\cdot CH_2Cl_2$ (**10**). The molecular structures of (**8**)—(**10**) have been established by single-crystal *X*-ray diffraction studies. The structures of both (**8**) and (**9**) consist of WFe_2 triangles of metal atoms with W–Fe and Fe–Fe bonds bridged by μ-PPh_2 ligands. The iron atoms all have two terminal CO ligands and the tungsten atoms are ligated by one CO ligand and a C_5H_5 group. In addition a W–Fe bond in complex (**8**) is semibridged by a CO ligand [Fe(2)–C(1) 1.791(7) Å, Fe(2)–C(1)–O(1) 159.4(8)°]. In compound (**8**) the metal triangle is capped by a μ_3-CR group [W–μ-CR 2.085(6), Fe–μ-CR 1.989(6) and 2.052(6) Å]. In contrast, the metal triangle in (**9**) is capped by a μ_3-$OCCH_2R$ moiety which is η^2 bound to the tungsten atom with σ attachments to the two iron atoms [W–O 2.129(6), W–C 2.155(7), Fe(1)–C 1.913(10), and Fe(2)–O 2.011(6) Å]. Formation of complex (**9**) from (**1**) involves the transfer of two hydrogen atoms from terminal PPh_2H ligands to the μ_3-CR ligand, followed by migration of the resulting μ-CH_2R group to metal-bound CO. The structure of (**10**) consists of a W–Fe(2)–Fe(1) chain of metal atoms which arises *via* cleavage of a W–Fe bond in (**1**). The W–Fe(2) and Fe(2)–Fe(1) bonds are bridged by μ-PPh_2 ligands and a PPh_2H ligand is attached to Fe(1). The tungsten atom carries two CO ligands and a C_5H_5 group, and each iron atom has two terminal CO ligands. The Fe–Fe bond is bridged by a μ-$OCCH_2R$ group [Fe(2)–O 2.038(3), Fe(1)–C 1.936(4) Å]. The spectroscopic data (i.r. and ^1H, ^{13}C-$\{^1H\}$, and ^{31}P-$\{^1H\}$ n.m.r.) for the new WFe_2 complexes are discussed and mechanisms are proposed to account for their formation.

The reaction of di- and higher nuclearity metal carbonyl complexes with secondary phosphines (PR_2H, R = alkyl or aryl) provides a useful synthetic route to new phosphido-bridged species.[1] The heterometallic alkylidyne clusters $[WFe_2(\mu_3\text{-}CR)(\mu\text{-}CO)(CO)_8(\eta\text{-}C_5H_5)]$, $[MCo_2(\mu_3\text{-}CR)(CO)_8(\eta\text{-}C_5H_5)]$ (M = Mo or W), $[WReCo_2(\mu_3\text{-}CR)(CO)_{15}]$, and $[ReCo_2(\mu_3\text{-}CR)(CO)_{10}]$ react with secondary phosphine ligands under particularly mild conditions, allowing the systematic synthesis of mono, bis, and tris phosphido bridged derivatives.[2,3]

---

† *Supplementary data available:* see Instructions for Authors, *J. Chem. Soc., Dalton Trans.*, 1990, Issue 1, pp. xix—xxii.

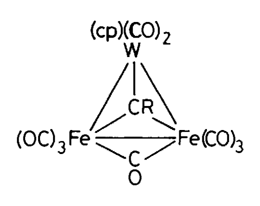

(1)

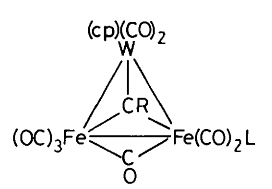

L
(2) PMe_2Ph
(3) PEt_2H

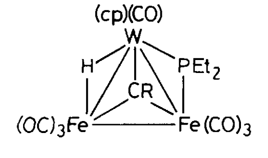

(4a)

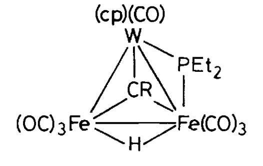

(4b)

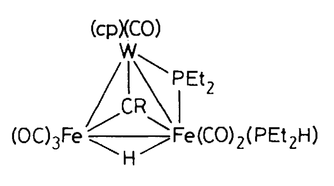

(5)

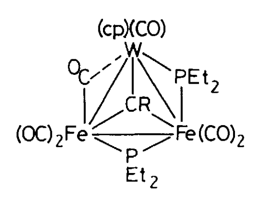

(6)

R = C_6H_4Me-4, cp = η - C_5H_5

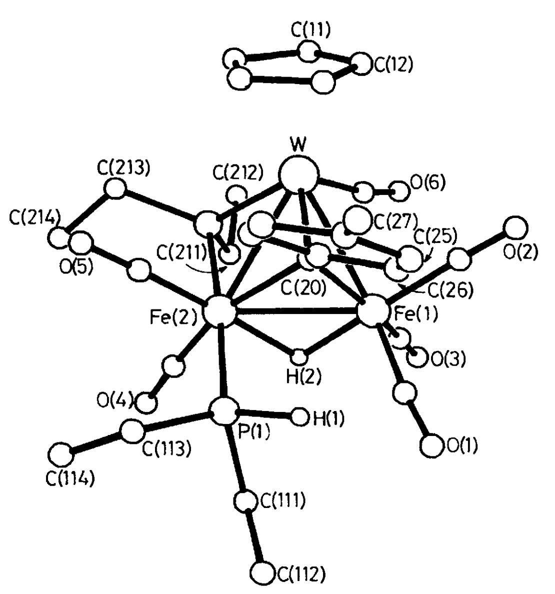

Figure 1. Molecular structure of $[WFe_2(\mu_3\text{-}CC_6H_4Me\text{-}4)(\mu\text{-}H)(\mu\text{-}PEt_2)(CO)_6(PEt_2H)(\eta\text{-}C_5H_5)]\cdot Et_2O$ **(5)** showing the atom numbering scheme

Herein we report reactions of the complex $[WFe_2(\mu_3\text{-}CR)(\mu\text{-}CO)(CO)_8(\eta\text{-}C_5H_5)]$ with secondary phosphine ligands PR'_2H (R′ = Ph or Et) which afford new phosphido bridged alkylidyne and acyl complexes. A preliminary account of some of this work has previously been published.[3]

Results and Discussion

The complex $[WFe_2(\mu_3\text{-}CR)(\mu\text{-}CO)(CO)_8(\eta\text{-}C_5H_5)]$ **(1)**; R = C_6H_4Me-4) has been shown to react with 2 equivalents of PMe_2Ph affording the bis(phosphine) derivative $[WFe_2(\mu_3\text{-}CR)(\mu\text{-}CO)(CO)_6(PMe_2Ph)_2(\eta\text{-}C_5H_5)]$.[4] Similarly, treatment of **(1)** with 1 equivalent of the bidentate phosphine $Ph_2PCH_2PPh_2$ (dppm) gave $[WFe_2(\mu_3\text{-}CR)(\mu\text{-}CO)(CO)_6(dppm)(\eta\text{-}C_5H_5)]$.[4] We now find that treatment of **(1)** with a single equivalent of PMe_2Ph in diethyl ether affords, after chromatography, good yields of the monosubstituted PMe_2Ph complex **(2)**. Moreover, the related reaction with PEt_2H gives the terminal secondary phosphine complex **(3)**. The spectroscopic and analytical data for complexes **(2)** and **(3)** are given in Tables 1—3. Their $^{31}P\text{-}\{^1H\}$ n.m.r. spectra show singlet resonances at δ 26.3 **(2)** and 48.6 p.p.m. **(3)** and the absence of ^{183}W satellite peaks on these signals confirms that the phosphine ligands ligate iron atoms in both complexes. The proton-coupled ^{31}P n.m.r. spectrum of **(3)** appears as a doublet at δ 48.6 p.p.m. and the large $J(PH)$ coupling of 366 Hz confirms the presence of the PEt_2H proton. The $^{13}C\text{-}\{^1H\}$ n.m.r. spectra showed the expected resonances for the ligated carbon atoms of the μ_3-*C*R ligands and in both complexes the carbonyl ligands gave rise to a single broad resonance which indicates dynamic behaviour of the type found in the parent complex **(1)**.[4]

At 20 °C solutions of complex **(3)** slowly lose carbon monoxide (1—2 d) and following chromatography good yields of the phosphido-bridged complex **(4)** are obtained. In solution **(4)** exists as an equilibrium mixture of two isomers [**(4a)**:**(4b)** 6:1] in which the hydride ligand bridges either a W–Fe **(4a)** or an Fe–Fe **(4b)** bond. At temperatures up to 80 °C sharp resonances are observed for both isomers in the n.m.r. spectra of **(4)**. Evidently, interconversion of **(4a)** and **(4b)** *via* hydride migration is slow on the n.m.r. time-scale at these temperatures. When crystals of **(4)** are dissolved in CH_2Cl_2, n.m.r. spectra of the freshly prepared solution show diminished proportions of isomer **(4b)**, and it requires *ca.* 4 h at room temperature for equilibrium to become established. This confirms that isomers **(4a)** and **(4b)** do slowly interconvert in solution and suggests that **(4a)** is the preferred isomer in the crystalline state.

Spectroscopic data for **(4a)** and **(4b)** are in accord with the structures shown. The $^{31}P\text{-}\{^1H\}$ n.m.r. spectrum has resonances at δ 162.8 [J(WP) 286 Hz] and 157.3 p.p.m. [J(WP) 366 Hz], which may be assigned to the $W(\mu\text{-}PEt_2)Fe$ moieties in **(4a)** and **(4b)** respectively. The ^1H n.m.r. spectrum was particularly informative showing doublet resonances at δ −16.03 [J(PH) 31, J(WH) 34 Hz] and −24.72 [J(PH) 15 Hz], which may be assigned to the hydride ligands bridging the W–Fe **(4a)** and Fe–Fe **(4b)** bonds. In **(4a)** and **(4b)** the μ-PEt_2 groups bridge heteronuclear W–Fe bonds. In contrast the rearrangement of the related complexes $[WCo_2(\mu_3\text{-}CR)(CO)_7(PR'_2H)(\eta\text{-}C_5H_5)]$ (R′ = Ph or Et) affords the compounds $[WCo_2(\mu_3\text{-}CR)(\mu\text{-}H)(\mu\text{-}PR'_2)(CO)_6(\eta\text{-}C_5H_5)]$, in which the homonuclear Co–Co bonds are bridged by the μ-PR'_2 ligands.[2a,b]

Addition of excess of PEt_2H (*ca.* 5 equivalents) to a CH_2Cl_2 solution of **(1)** (12 h, 20 °C) affords a deep purple-red solution and following chromatography red crystals of complex **(5)** were obtained in good yield. The structure of **(5)** was established by a single-crystal *X*-ray diffraction study. The results are summarized in Table 4 and the molecular structure is shown in Figure 1. The compound has the expected triangular WFe_2 core which is capped by a μ_3-alkylidyne ligand. The M–M and M–μ_3-C separations [W–Fe(1) 2.763(1), W–Fe(2) 2.830(1), Fe(1)–Fe(2) 2.687(2), W–μ-C 2.042(8), Fe(1)–μ-C 1.960(8), and

Table 1. Analytical[a] and physical data for the tungsten–iron complexes

Compound[b]	Colour	Yield (%)	$\tilde{\nu}$(CO)[c]/cm^{-1}	Analysis (%)	
				C	H
(2) $[\mathrm{WFe_2(\mu_3\text{-}CR)(\mu\text{-}CO)(CO)_7(PMe_2Ph)(\eta\text{-}C_5H_5)}]$	Brown	88	2 045w, 2 034m, 1 994s, 1 972s, 1 945m, 1 893w(br), 1 789w(br)	42.2(42.2)	2.9(2.8)
(3) $[\mathrm{WFe_2(\mu_3\text{-}CR)(\mu\text{-}CO)(CO)_7(PEt_2H)(\eta\text{-}C_5H_5)}]$	Brown	63	[d]2 037m, 2 001s, 1 971s, 1 947w, 1 939w, 1 855w, 1 816w(br), 1 792w(br)	38.3(38.6)	2.8(3.0)
(4) $[\mathrm{WFe_2(\mu_3\text{-}CR)(\mu\text{-}H)(\mu\text{-}PEt_2)(CO)_7(\eta\text{-}C_5H_5)}]$	Black	67	[e]2 050s, 2 007s, 1 988s, 1 969s, 1 962m, 1 942m	38.3(38.4)	3.1(3.1)
(5) $[\mathrm{WFe_2(\mu_3\text{-}CR)(\mu\text{-}H)(PEt_2)(CO)_6(PEt_2H)(\eta\text{-}C_5H_5)}]$[f]	Orange-red	53	[e]2 023s, 1 986s, 1 962m, 1 937s, 1 824m	42.5(42.0)	4.8(5.0)
(6) $[\mathrm{WFe_2(\mu_3\text{-}CR)(\mu\text{-}PEt_2)_2(CO)_6(\eta\text{-}C_5H_5)}]$	Dark brown	69	[g]2 016s, 1 968s, 1 954s, 1 922s, 1 898w	39.8(40.0)	4.0(4.0)
(7) $[\mathrm{WFe_2(\mu_3\text{-}CR)(\mu\text{-}H)(\mu\text{-}PPh_2)(CO)_7(\eta\text{-}C_5H_5)}]$	Olive green	73	[e]2 051s, 2 012s, 1 992s, 1 977m, 1 967m, 1 944m	45.9(45.4)	3.2(2.7)
(8) $[\mathrm{WFe_2(\mu_3\text{-}CR)(\mu\text{-}PPh_2)_2(CO)_6(\eta\text{-}C_5H_5)}]$[h]	Green	87	2 018s, 1 972s, 1 950s, 1 930s, 1 884w(br)	49.7(50.0)	3.2(3.2)
(9) $[\mathrm{WFe_2(\mu_3\text{-}OCCH_2R)(\mu\text{-}PPh_2)_2(CO)_5(\eta\text{-}C_5H_5)}]$	Black	50	2 007s, 1 970s, 1 951m, 1 916m, 1 785w(br)	51.3(51.4)	3.3(3.4)
(10) $[\mathrm{WFe_2(\mu\text{-}OCCH_2R)(\mu\text{-}PPh_2)_2(CO)_6(PPh_2H)(\eta\text{-}C_5H_5)}]$[i]	Dark brown	22	[j]1 992s, 1 961s, 1 933s, 1 915m, 1 904m, 1 835m	52.4(52.5)	3.6(3.6)

[a] Calculated values are given in parentheses. [b] R = C_6H_4Me-4. [c] In CH_2Cl_2 unless otherwise stated. [d] In Et_2O. [e] In methylcyclohexane. [f] Crystallized with one Et_2O. [g] In hexane. [h] Crystallized with 0.5 CH_2Cl_2. [i] Crystallized with one CH_2Cl_2. [j] Weak acyl CO absorption at 1 480 cm^{-1}.

Table 2. Hydrogen-1 and carbon-13 n.m.r. data[a] for complexes

Compound	^{1}H(δ)[b]	^{13}C(δ)[c]
(2)	1.87 [d, 6 H, PMe_2Ph, *J*(PH) 9], 2.36 (s, 3 H, Me-4), 5.30 (s, 5 H, C_5H_5), 7.09, 7.34 [(AB)$_2$, 4 H, C_6H_4, *J*(HH) 8], 7.5 (m, 5 H, Ph)	270.4 [μ_3-*C*R, *J*(WC) 88], 218.2 (s, br, 8 CO), 160.2 [C^1(C_6H_4)], 138.1 [d, C^1(Ph), *J*(PC) 44], 136.2 [C^4(C_6H_4)], 128—132 (C_6H_4, Ph), 91.4 (C_5H_5), 21.2 (Me-4), 16.8 [d, PMe_2Ph, *J*(PC) 15], 16.2 [d, PMe_2Ph, *J*(PC) 15]
(3)	0.8—2.4 (m, br, 10 H, PEt_2H), 2.38 (s, 3 H, Me-4), 4.00 [d, br, 1 H, PEt_2*H*, *J*(PH) 366], 5.28 (s, C_5H_5), 7.13, 7.30 [(AB)$_2$, 4 H, C_6H_4, *J*(HH) 8]	[d]275.0 (s, μ_3-*C*R), 216.0 (s, br, 8 CO), 160.3 [C^1(C_6H_4)], 136.7 [C^4(C_6H_4)], 132.0 [C^2,C^6(C_6H_4)], 128.6 [C^3,C^5(C_6H_4)], 89.5 (C_5H_5), 21.2 (Me-4), 15.8 [d, *C*H_2Me, *J*(PC) 28], 14.2 [d, *C*H_2Me, *J*(PC) 28], 11.4 [d, CH_2*Me*, *J*(PC) 9], 9.0 (CH_2*Me*)
(4)	[e]$-$24.72* [d, 1 H, Fe_2(μ-H), *J*(PH) 15], $-$16.03 [d, 1 H, WFe(μ-H), *J*(PH) 31, *J*(WH) 34], 1.1—2.4 (m, 10 H, μ-PEt_2), 2.35 (s, 3 H, Me-4), 5.22 (s, 5 H, C_5H_5), 7.08, 7.28 [(AB)$_2$, 4 H, C_6H_4, *J*(HH) 8]	262.7 [μ_3-*C*R, *J*(WC) 110], 213.7 [Fe(CO)$_3$], 213.3 [d, WCO, *J*(PC) 9, *J*(WC) 162], 213.0 [s, br, Fe(CO)$_3$], 162.2 [C^1(C_6H_4)], 134.9 [C^4(C_6H_4)], 128.6 [C^2,C^6(C_6H_4)], 127.6 [C^3,C^5(C_6H_4)], 87.6 (s, C_5H_5), 29.8 [d, *C*H_2Me, *J*(PC) 28], 24.3 [d, *C*H_2Me, *J*(PC) 24], 21.2 (Me-4), 14.5 [d, CH_2*Me*, *J*(PC) 9], 12.6 (CH_2*Me*)
(5)	$-$25.38 [dd, 1 H, Fe_2(μ-H), *J*(PH) 24, 11], 0.8—3.0 (m, 20 H, μ-PEt_2, PEt_2H), 2.32 (s, 3 H, Me-4), 3.7 [dd, br, 1 H, PEt_2*H*, *J*(PH) 369, 10], 5.16 (s, 5 H, C_5H_5), 7.0—7.5 (m, br, 4 H, C_6H_4)	[f]256.6 [μ_3-*C*R, *J*(WC) 100], 225.4 [d, WCO, *J*(PC) 7, *J*(WC) 172], 216.3 [dd, FeCO, *J*(PC) 20, 20], 215.1 (FeCO), 214.8 (FeCO), 211.7 [d, FeCO, *J*(PC) 15], 209.9 [dd, FeCO, *J*(PC) 24, 10], 162.7 [C^1(C_6H_4)], 133.8 [C^4(C_6H_4)], 129.8 [br, C^2,C^6(C_6H_4)], 128.4 [C^3,C^5(C_6H_4)], 92.6 (C_5H_5), 31.8 [d, *C*H_2Me, *J*(PC) 22], 26.3 [d, *C*H_2Me, *J*(PC) 25], 21.1 (Me-4), 19.3 [d, *C*H_2Me, *J*(PC) 29], 14.7 [d, *C*H_2Me, *J*(PC) 27], 12.4 [d, CH_2*Me*, *J*(PC) 7], 12.0 [d, CH_2*Me*, *J*(PC) 10], 11.6 (CH_2*Me*), 8.0 (CH_2*Me*)
(6)	1.1—1.6 (m, 12 H, CH_2*Me*), 1.6—3.1 (m, 8 H, *C*H_2Me), 2.21 (s, 3 H, Me-4), 4.93 [d, 5 H, C_5H_5, *J*(PH) 1], 6.38, 6.77 [(AB)$_2$, 4 H, C_6H_4, *J*(HH) 8]	220.5 [dd, FeCO, *J*(PC) 20, 12], 217.3 [d, WCO, *J*(PC) 10, *J*(WC) 147], 216.9 [dd, μ_3-*C*R, *J*(PC) 37, 12, *J*(WC) 107], 215.0 [br, Fe(CO)$_3$], 209.5 [dd, FeCO, *J*(PC) 12, 12], 161.5 [C^1(C_6H_4)], 133.8 [C^4(C_6H_4)], 128.5 [C^2,C^6(C_6H_4)], 127.7 [C^3,C^5(C_6H_4)], 92.4 (C_5H_5), 32.2 [d, *C*H_2Me, *J*(PC) 20], 28.5 [d, *C*H_2Me, *J*(PC) 10], 27.4 [d, *C*H_2Me, *J*(PC) 29], 20.9 (Me-4), 19.5 [d, *C*H_2Me, *J*(PC) 24], 12.6 [d, CH_2*Me*, *J*(PC) 7], 11.4 [d, CH_2*Me*, *J*(PC) 7], 11.3 [d, CH_2*Me*, *J*(PC) 7], 11.0 [d, CH_2*Me*, *J*(PC) 5]
(7)	$-$15.90 [d, 1 H, WFe(μ-H), *J*(PH) 33, *J*(WH) 33], 2.36 (s, 3 H, Me-4), 5.46 (s, 5 H, C_5H_5), 7.0—8.0 (m, 14 H, Ph, C_6H_4)	270.5 [μ_3-*C*R, *J*(WC) 110], 213.5 [Fe(CO)$_3$], 212.4 [s, br, Fe(CO)$_3$], 211.1 [d, WCO, *J*(PC) 9, *J*(WC) 164], 161.5 [C^1(C_6H_4)], 143.0—128.0 (Ph, C_6H_4), 88.8 (C_5H_5), 21.2 (Me-4)
(8)	2.13 (s, 3 H, Me-4), 5.20 (s, 5 H, C_5H_5), 6.09, 6.39 [(AB)$_2$, 4 H, C_6H_4, *J*(HH) 8], 6.7—8.0 (m, 20 H, Ph)	220.6 [dd, FeCO, *J*(PC) 20, 20], 214.0 [s, br, Fe(CO)$_3$], 212.6 (WCO), 212.2 [dd, μ_3-*C*R, *J*(PC) 38, 15], 210.4 [dd, FeCO, *J*(PC) 9, 9], 169.5 [C^1(C_6H_4)], 147.0—127.0 (Ph, C_6H_4), 94.5 (C_5H_5), 20.8 (Me-4)
(9)	2.23 (s, 3 H, Me-4), 3.43 [AB$_q$, 2 H, CH_2R, *J*(HH) 16], 4.85 (s, 5 H, C_5H_5), 6.77, 6.89 [(AB)$_2$, 4 H, C_6H_4, *J*(HH) 8], 7.0—8.2 (m, 20 H, Ph)	[g]258.8 (μ_3-O*C*CH_2R), 219.7 [d, CO, *J*(PC) 7], 217.5 (CO), 217.0 [dd, FeCO, *J*(PC) 12, 12], 209.8 [dd, FeCO, *J*(PC) 13, 13], 197.2 [d, CO, *J*(PC) 12], 143.0—128.0 (m, Ph, C_6H_4), 89.4 (C_5H_5), 21.2 (Me-4)
(10)	2.07 (s, 3 H, Me-4), 4.29 [AB$_q$, 2 H, CH_2R, *J*(HH) 17], 4.45 [dd, 1 H, PPh_2*H*, *J*(PH) 354, 11], 4.61 (s, 5 H, C_5H_5), 6.2—7.6 (m, 34 H, Ph, C_6H_4)	294.4 [dd, μ-O*C*CH_2R, *J*(PC) 25, 18], 234.6 [dd, FeCO, *J*(PC) 18 18], 232.7 [d, CO, *J*(PC) 18], 227.7 [WCO, *J*(WC) 178], 219.7 (br, CO), 217.1 [dd, FeCO, *J*(PC) 21, 21], 212.8 [ddd, FeCO, *J*(PC) 18, 9, 9], 145.0—124.0 (m, Ph, C_6H_4), 91.8 (C_5H_5), 66.7 [d, OC*C*H_2R, *J*(PC) 9], 21.0 (Me-4)

[a] Chemical shifts (δ) in p.p.m., coupling constants in Hz. [b] Measured in CD_2Cl_2 at room temperature. [c] Hydrogen-1 decoupled, measured in CD_2Cl_2—CH_2Cl_2 unless otherwise noted, chemical shifts to high frequency of $SiMe_4$. [d] Measured at 0 °C. [e] The resonance for the minor isomer (**4b**) is marked with an asterisk, other peaks for this isomer could not be assigned. [f] Measured at $-$30 °C. [g] Measured at $-$50 °C; a room-temperature spectrum in $CDCl_3$—$CHCl_3$ revealed the μ_3-OC*C*H_2R resonance at δ 53.5 p.p.m.

Fe(2)–μ-C 2.104(8) Å] are comparable with those found for a series of closely related complexes, data for which are summarized in Table 5. The W–Fe(2) bond is bridged by a μ-PEt$_2$ group [W–P(2) 2.311(2) and Fe(2)–P(2) 2.315(3) Å] and a hydride ligand symmetrically bridges the Fe–Fe bond [Fe(1)–H(2) 1.67(10) and Fe(2)–H(2) 1.74(9) Å]. One iron atom carries three approximately orthogonal terminal carbonyl ligands, whilst the other has two terminal CO ligands and a terminal PEt$_2$H ligand which is *trans* to the μ-PEt$_2$ group [P(1)–Fe(2)–P(2) 174.3(1)°]. The PEt$_2$*H* hydrogen atom was also located in the *X*-ray study and has a P–H separation [1.46(9) Å] which is identical within error to that found in [Co$_2$(μ-PPh$_2$)$_2$(CO)$_4$(PPh$_2$H)$_2$][P–H 1.45(14) Å].[5] The μ-H and P–H hydrogen atoms are separated by 3.16(10) Å, and their relatively close proximity may facilitate the thermally induced loss of H$_2$ from this complex which is discussed in a following section.

Spectroscopic data for complex (**5**) are in accord with the solid-state structure being maintained in solution. The ^{1}H n.m.r. spectrum has a resonance at δ −25.38 p.p.m. [dd, *J*(PH) 24, 11 Hz] which is assigned to the Fe$_2$(μ-H) moiety and the presence of the terminal PEt$_2$H ligand is confirmed by the observation of a broad resonance for the P–H proton at δ 3.7 p.p.m. [dd, *J*(PH) 369, 10 Hz]. The resonances for the C$_6$*H*$_4$Me-4 protons were unusually broad and it is possible that steric hindrance from the PEt$_2$H ligand results in restricted rotation of the C$_6$H$_4$Me-4 ring about the C(20)–C(21) bond.The ^{31}P-{^{1}H} n.m.r. spectrum shows signals due to the Fe(PEt$_2$H) ligand [δ 43.0 p.p.m., d, *J*(PP) 42 Hz] and the WFe(μ-PEt$_2$) group [δ 164.5 p.p.m., d, *J*(PP) 42, *J*(WP) 366 Hz]. The relatively large P–P coupling is consistent with the *trans* orientation of these ligands found in the solid-state structure and the observation of ^{183}W satellite peaks on the latter resonance confirms that the W–Fe(2) bond is bridged by the μ-PEt$_2$ ligand.

Table 3. Phosphorus-31 n.m.r. data for the complexes[a]

Compound	
(**2**)	26.3 (s, PMe$_2$Ph)
(**3**)	[b] 48.6 [d, br, PEt$_2$H, *J*(PH) 366]
(**4a**)	162.8 [s, WFe(μ-P), *J*(WP) 286]
(**4b**)	157.3 [s, WFe(μ-P), (WP) 366]
(**5**)	43.0 [d, Fe(PEt$_2$H), *J*(PP) 42], 164.5 [d, WFe(μ-P), *J*(PP) 42, *J*(WP) 366]
(**6**)	196.3 [d, WFe(μ-P), *J*(PP) 17, *J*(WP) 317], 218.9 [d, Fe$_2$(μ-P), *J*(PP) 17]
(**7**)	156.3 [s, WFe(μ-P), *J*(WP) 298]
(**8**)	186.8 [d, WFe(μ-P), *J*(PP) 20, *J*(WP) 332], 199.4 [d, Fe$_2$(μ-P), *J*(PP) 20]
(**9**)	120.2 [d, WFe(μ-P), *J*(PP) 58, *J*(WP) 308], 227.4 [d, Fe$_2$(μ-P), *J*(PP) 58]
(**10**)	44.0 [dd, Fe(PPh$_2$H), *J*(PP) 27, 5], 154.4 [dd, WFe(μ-P), *J*(PP) 29, 5, *J*(WP) 303], 192.1 [dd, Fe$_2$(μ-P), *J*(PP) 29, 27]

[a] Chemical shifts in p.p.m., coupling constants in Hz, Hydrogen-1 decoupled unless otherwise stated; chemical shifts are positive to high frequency of 85% H$_3$PO$_4$ (external), measured in CD$_2$Cl$_2$. [b] Hydrogen-1 coupled.

The mechanism by which complex (**5**) is formed from (**1**) and excess of PEt$_2$H was examined in more detail by monitoring the reaction by i.r. spectroscopy and thin-layer chromatography. Initially rapid attack (*ca.* 10 min) of PEt$_2$H on (**1**) gives the terminal phosphine derivative (**3**). There was no evidence for the formation of a bis(phosphine) complex [WFe$_2$(μ_3-CR)(μ-CO)(CO)$_6$(PEt$_2$H)$_2$(η-C$_5$H$_5$)] analogous to the bis-PMe$_2$Ph complex [WFe$_2$(μ_3-CR)(μ-CO)(CO)$_6$(PMe$_2$Ph)$_2$(η-C$_5$H$_5$)]. This may be because the strongly σ-donating PEt$_2$H ligand in (**3**) deactivates the cluster towards further carbonyl substitution. Further monitoring of the reaction revealed the formation of the μ-PEt$_2$ complex (**4**) from (**3**). This rearrangement was qualitatively observed to proceed more rapidly in the presence of excess of PEt$_2$H, and free PEt$_2$H is evidently capable of acting as a Lewis-base catalyst for the transfer of a hydrogen atom from a PEt$_2$H ligand to a metal–metal bond. Base-catalysed transformation of [Os$_3$(CO)$_{11}$(PRR′H)] to [Os$_3$(μ-H)(μ-PRR′)(CO)$_{10}$] has previously been reported.[1a] As (**4**) is formed, further attack of PEt$_2$H gives (**5**). Interestingly, the latter complex is completely stable in the presence of PEt$_2$H. Presumably the PEt$_2$*H* proton in (**5**) is less acidic than the equivalent atom in (**3**), and (**5**) is therefore no longer susceptible to PEt$_2$H-catalysed rearrangement to a bis(μ-PEt$_2$) species such as (**6**).

Thermolysis of (**5**) in refluxing toluene (111 °C) results in loss of dihydrogen and formation of the bis(μ-PEt$_2$) complex (**6**). The ^{31}P-{^{1}H} n.m.r. spectrum of (**6**) shows two doublets at δ 196.3 [*J*(PP) 17, *J*(WP) 317 Hz] and 218.9 p.p.m. [*J*(PP) 17 Hz] and these may be assigned to μ-PEt$_2$ groups bridging the W–Fe and Fe–Fe bonds respectively. In the ^{13}C-{^{1}H} n.m.r. spectrum the μ_3-C resonance appears at δ 216.9 p.p.m. [dd, *J*(PC) 37, 12, *J*(WC) 107 Hz]. This is appreciably more shielded than found in the complexes (**1**) (δ 282.6), (**3**) (δ 275.0), or (**4a**) (δ 262.7 p.p.m.)

Table 4. Selected internuclear distances (Å) and angles (°) for [WFe$_2$(μ_3-CC$_6$H$_4$Me-4)(μ-H)(μ-PEt$_2$)(CO)$_6$(PEt$_2$H)(η-C$_5$H$_5$)] (**5**) with estimated standard deviations (e.s.d.s) in parentheses

W–Fe(1)	2.763(1)	W–Fe(2)	2.830(1)	W–P(2)	2.311(2)	W–C(6)	1.94(1)
W–C(20)	2.042(8)	Fe(1)–Fe(2)	2.687(2)	Fe(1)–H(2)	1.67(10)	Fe(1)–C(1)	1.792(9)
Fe(1)–C(2)	1.78(1)	Fe(1)–C(3)	1.79(1)	Fe(1)–C(20)	1.960(8)	Fe(2)–P(1)	2.241(3)
Fe(2)–P(2)	2.315(3)	Fe(2)–H(2)	1.74(9)	Fe(2)–C(4)	1.768(9)	Fe(2)–C(5)	1.75(1)
Fe(2)–C(20)	2.104(8)	P(1)–H(1)	1.46(9)	C(1)–O(1)	1.14(1)	C(2)–O(2)	1.14(1)
C(3)–O(3)	1.14(1)	C(4)–O(4)	1.15(1)	C(5)–O(5)	1.16(1)	C(6)–O(6)	1.18(1)
Fe(1)–W–Fe(2)	57.4(1)	Fe(1)–W–P(2)	91.2(1)	Fe(2)–W–P(2)	52.3(1)	Fe(1)–W–C(20)	45.1(2)
Fe(2)–W–C(20)	47.9(2)	P(2)–W–C(20)	100.2(2)	C(6)–W–C(20)	112.1(3)	W–Fe(1)–Fe(2)	62.6(1)
W–Fe(1)–H(2)	95(3)	Fe(2)–Fe(1)–H(2)	39(3)	C(1)–Fe(1)–C(2)	93.4(4)	C(1)–Fe(1)–C(3)	98.9(4)
C(2)–Fe(1)–C(3)	96.2(5)	W–Fe(1)–C(20)	47.6(2)	Fe(2)–Fe(1)–C(20)	51.0(2)	H(2)–Fe(1)–C(20)	88(3)
W–Fe(2)–Fe(1)	60.0(1)	W–Fe(2)–P(1)	133.5(1)	Fe(1)–Fe(2)–P(1)	90.3(1)	W–Fe(2)–P(2)	52.2(1)
Fe(1)–Fe(2)–P(2)	93.0(1)	P(1)–Fe(2)–P(2)	174.3(1)	W–Fe(2)–H(2)	92(3)	Fe(1)–Fe(2)–H(2)	37(3)
P(1)–Fe(2)–H(2)	80(3)	P(2)–Fe(2)–H(2)	100(3)	P(1)–Fe(2)–C(4)	90.3(3)	P(1)–Fe(2)–C(5)	92.1(3)
C(4)–Fe(2)–C(5)	99.9(4)	W–Fe(2)–C(20)	46.0(2)	Fe(1)–Fe(2)–C(20)	46.3(2)	P(1)–Fe(2)–C(20)	87.4(2)
P(2)–Fe(2)–C(20)	98.2(2)	H(2)–Fe(2)–C(20)	82(3)	Fe(2)–P(1)–H(1)	115(4)	W–P(2)–Fe(2)	75.4(1)
Fe(1)–H(2)–Fe(2)	104(5)	Fe(1)–C(1)–O(1)	174(1)	Fe(1)–C(2)–O(2)	178.3(7)	Fe(1)–C(3)–O(3)	176.8(8)
Fe(2)–C(4)–O(4)	177.1(8)	Fe(2)–C(5)–O(5)	177.5(8)	W–C(6)–O(6)	169.8(7)	W–C(20)–Fe(1)	87.3(3)
W–C(20)–Fe(2)	86.1(3)	Fe(1)–C(20)–Fe(2)	82.7(3)	W–C(20)–C(21)	130.7(5)	Fe(1)–C(20)–C(21)	128.7(5)
Fe(2)–C(20)–C(21)	125.7(7)						

Table 5. Bond length (Å) data for closely related WFe_2 complexes

Compound[a]	W–Fe	Fe–Fe	W–μ-C	Fe–μ-C	W–μ-P	Fe–μ-P
$[WFe_2(\mu_3\text{-}CR)(\mu\text{-}CO)(CO)_8(\eta\text{-}C_5H_5)]$ (**1**)[b]	2.756(2) 2.805(2)	2.538(2)	2.093(5)	1.969(5) 2.036(5)		
$[WFe_2(\mu_3\text{-}CR)(\mu\text{-}H)(\mu\text{-}PEt_2)(CO)_6(PEt_2H)(\eta\text{-}C_5H_5)]$ (**5**)[c]	2.763(1) 2.830(1)[d]	2.687(2)[e]	2.042(8)	1.960(8) 2.104(8)	2.311(2)	2.315(3)
$[WFe_2(\mu_3\text{-}CR)(\mu\text{-}PPh_2)_2(CO)_6(\eta\text{-}C_5H_5)]$ (**8**)[c]	2.735(1)[d] 2.783(1)	2.572(1)[d]	2.085(6)	1.989(6) 2.052(6)	2.363(2)	2.194(2) 2.229(2) 2.248(2)
$[WFe_2(\mu_3\text{-}OCCH_2R)(\mu\text{-}PPh_2)_2(CO)_5(\eta\text{-}C_5H_5)]$ (**9**)[c]	2.712(1)[d] 2.723(1)	2.616(2)[d]			2.412(2)	2.149(3) 2.255(2) 2.256(2)
$[WFe_2(\mu\text{-}OCCH_2R)(\mu\text{-}PPh_2)_2(CO)_6(PPh_2H)(\eta\text{-}C_5H_5)]$ (**10**)[c]	2.940(1)[d]	2.667(1)[d]			2.392(1)	2.213(1) 2.232(1) 2.270(1)
$[WFe_2(\mu_3\text{-}CR)(\mu\text{-}H)(\mu\text{-}PPh_2)(CO)_6(\eta\text{-}C_5H_5)]$[f,g]	2.523(1)[d] 2.817(1)	2.569(1)[e]	2.018(4)	1.916(5) 2.132(3)	2.357(1)	2.219(1)
$[WFe_2(\mu_3\text{-}CR)\{\mu\text{-}C(O)C(Me)CHMe\}(\mu\text{-}PEt_2)(CO)_5(\eta\text{-}C_5H_5)]$[f]	2.679(1) 2.808(1)[d]	2.673(1)	1.992(5)	2.025(5) 2.130(5)	2.374(2)	2.262(2)
$[WFe_2(\mu_3\text{-}CR)(\mu\text{-}PEt_2)_3(CO)_4(\eta\text{-}C_5H_5)]$[h,i]	2.714(1)[d] 2.722(1)[d]	2.569(1)[d]	1.981(5)	2.021(5) 2.081(5)	2.338(2) 2.341(2)	2.185(2) 2.198(2) 2.233(2) 2.250(2)
$[WFe_2(\mu_3\text{-}CR)H(\mu\text{-}PEt_2)_3(CO)_4(\eta\text{-}C_5H_5)]$[h]	2.770(1)[d] 2.796(1)[d]	2.576(1)[d]	2.040(5)	2.019(5) 2.068(5)	2.361(1) 2.375(1)	2.194(1) 2.197(1) 2.209(1) 2.210(2)

[a] R = C_6H_4Me-4. [b] Ref. 4. [c] This paper. [d] Bridged by a μ-P ligand. [e] Bridged by a μ-H ligand. [f] Ref. *3b*. [g] 46 Cluster valence electrons. [h] J. C. Jeffery and J. G. Lawrence-Smith, unpublished work. [i] 47 Cluster valence electron radical.

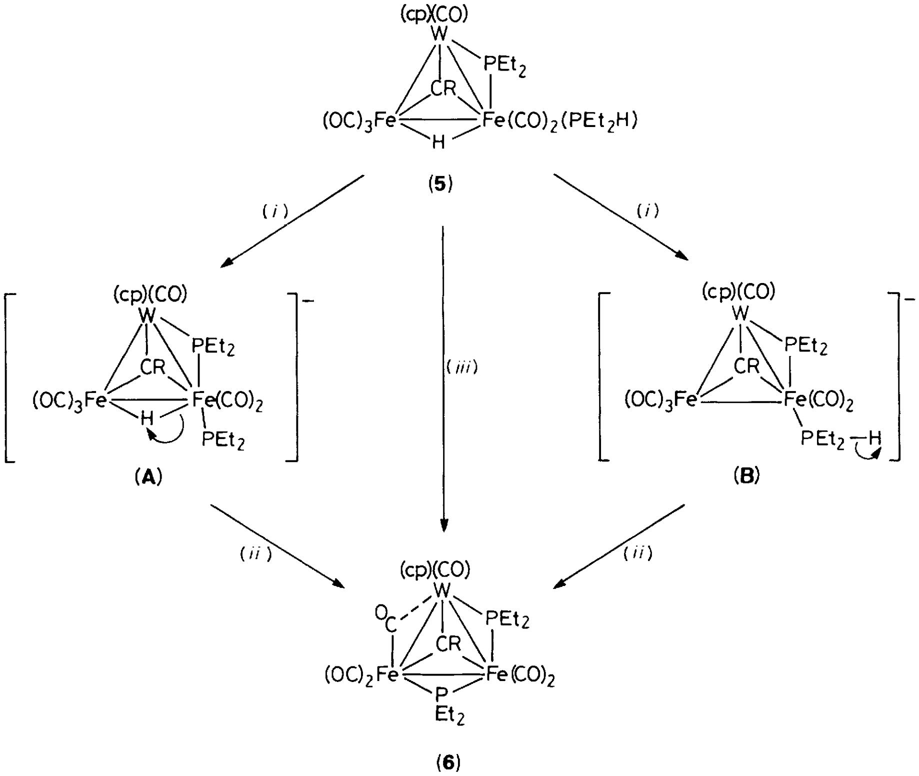

Scheme 1. R = C_6H_4Me-4. (*i*) $LiBEt_3H$, $+H^-$, $-H_2$; (*ii*) $-H^-$; (*iii*) 111 °C, toluene, $-H_2$

and lies in the region more normally associated with iron CO ligands. Fortunately a similarly shielded μ_3-C resonance at δ 212.2 p.p.m. is observed for the μ-PPh_2 analogue (**8**), and the structure of this complex has been confirmed by a single-crystal *X*-ray diffraction study (see following section).

Although free PEt_2H is not sufficiently basic to catalyse the conversion of complex (**5**) into (**6**), this transformation may be effected under mild conditions (20 °C) by the addition of 0.1 molar equivalents of $Li[BEt_3H]$. A plausible mechanism for this Lewis base-catalysed rearrangment is shown in Scheme 1.

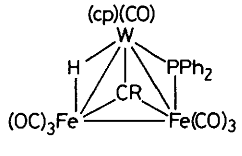

(7)

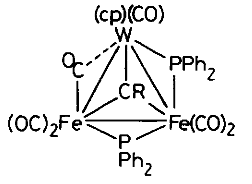

(8)

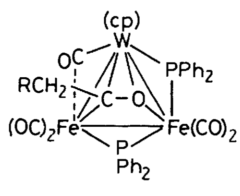

(9)

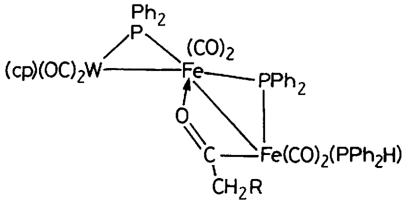

(10)

R = C_6H_4Me-4, cp = η-C_5H_5

Deprotonation of (**5**) could afford anionic intermediates such as (**A**) or (**B**) which could readily rearrange with loss of H^- to give (**6**)

The reactions of complex (**1**) with PPh_2H were also studied for comparison with those observed with PEt_2H. Treatment of (**1**) with 1 equivalent of PPh_2H in a dilute diethyl ether solution initially gave an orange-brown solution which became dark green over a period of *ca.* 3 h. I.r. spectroscopy suggests that the initial red-brown solution may contain a terminal PPh_2H species analogous to the PEt_2H complex (**3**). This red-brown intermediate could not be isolated because of the ease with which it rearranges to the stable dark green μ-PPh_2 bridged complex (**7**). Spectroscopic data for (**7**) show that it exists as a single isomer in solution having the same structure as the PEt_2H isomer (**4a**). Thus the ^{31}P-{^1H} n.m.r. spectrum shows a resonance at δ 156.3 p.p.m. for the μ-PPh_2 ligand and the presence of ^{183}W satellites [*J*(WP) 298 Hz] confirms that this ligand bridges a W–Fe bond. In the ^1H n.m.r. spectrum the μ-H resonance occurs at δ −15.90 [*J*(PH) 33, *J*(WH) 33 Hz]; these values are very similar to those observed for (**4a**) and confirm that the μ-H ligand bridges a W–Fe bond.

The reaction of complex (**1**) with an excess of PPh_2H was also investigated and gave results which were substantially different from those obtained with PEt_2H. The reaction is sensitive to the concentration of PPh_2H used. Treatment of (**1**) with *ca.* 3 equivalents of PPh_2H in CH_2Cl_2 gave a moderate yield (*ca.* 20%) of the bis(μ-PPh_2) complex (**8**), good yields (*ca.* 50%) of the μ_3-acyl complex (**9**), and traces (< 10%) of the μ-acyl complex (**10**). At higher concentrations of PPh_2H (> 5 equivalents in the minimum volume of solvent) the yield of (**9**) remains similar, and reduced yields (< 10%) of (**8**) and proportionately increased yields (*ca.* 20%) of (**10**) are observed. Spectroscopic data for (**8**)—(**10**) did not allow unambiguous assignment of their structures but fortunately the availability of crystals of these complexes allowed single-crystal *X*-ray diffraction studies to be carried out on all three species.

The structure of the bis(μ-PPh_2) complex (**8**) is shown in Figure 2 and selected bond lengths and angles are given in Table 6. The structure reveals the expected WFe_2 triangle of metal atoms capped by a μ_3-CC_6H_4Me-4 ligand. The Fe–Fe and one W–Fe bond are bridged by μ-PPh_2 ligands which are approximately coplanar with the metal atoms. The tungsten atom carries a terminal CO ligand and a cyclopentadienyl group. The W–Fe(2) bond is semi-bridged by a CO ligand attached to Fe(2) [Fe(2)–C(1) 1.791(7), W–C(1) 2.535(9) Å, Fe(2)–C(1)–O(1) 159.4(8)°] and both Fe atoms are ligated by two approximately orthogonal CO ligands. Comparison of the parameters of the μ_3-$CWFe_2$ core with those of the parent complex (**1**) (Table 5) shows that introduction of the μ-PPh_2 ligands leads to a contraction of the W–Fe and W–μ-C bonds and a proportional increase in the Fe–Fe and Fe–μ-C distances. Spectroscopic data for (**8**) are extremely similar to those of the μ-PEt_2 analogue (**6**). Further investigation revealed that (**8**) may be more efficiently prepared by treating the μ-PPh_2 bridged complex (**7**) with 1 equivalent of PPh_2H. Formation of (**8**) from (**1**) therefore proceeds *via* a series of intermediates similar to those involved in the formation of the μ-PEt_2 complex (**6**). The absence of isolable terminal PPh_2H complexes analogous to (**3**) and (**5**) emphasizes the ease with which terminal PPh_2H complexes rearrange to μ-PPh_2 species.

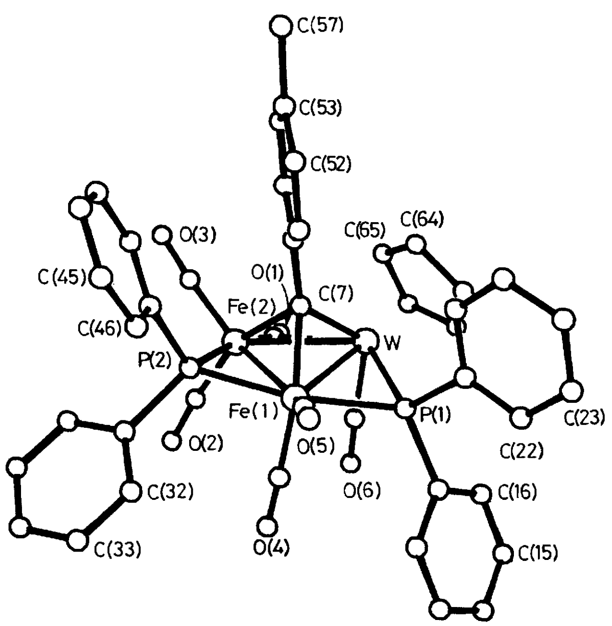

Figure 2. Molecular structure of $[WFe_2(\mu_3\text{-}CC_6H_4Me\text{-}4)(\mu\text{-}PPh_2)_2(CO)_6(\eta\text{-}C_5H_5)]\cdot0.5\ CH_2Cl_2$ (**8**) showing the atom numbering scheme

The major product obtained in the reaction of (**1**) with an excess of PPh_2H was the μ_3-acyl complex (**9**). The molecular structure of (**9**) is shown in Figure 3 and selected bond lengths and angles are in Table 7. The structure of (**9**) consists of a WFe_2 triangle of metal atoms with W–Fe and Fe–Fe bonds bridged by μ-PPh_2 ligands. The M–M and Fe–μ-P separations are unremarkable (Table 5), however the W–P(1) distance of 2.412(2) Å is the longest we have observed in complexes of this type (normal range W–μ-P 2.311—2.392 Å). Interest centres on the μ_3-acyl ligand which acts as a five-electron donor to the metal triangle. The RCH_2CO moiety is η^2-bound to tungsten [W–C(5) 2.155(7), W–O(5), 2.129(6) Å] with σ attachments to the two iron atoms [Fe(1)–C(5) 1.913(10), Fe(2)–O(5) 2.011(6) Å]. The co-ordination mode of this ligand is thus extremely similar to that observed in the complex $[WOs_3(\mu_3\text{-}OCCH_2C_6H_4Me\text{-}4)(CO)_{11}(\eta\text{-}C_5H_5)]$.[6] The acyl C(5)–O(5) distance of 1.43(1) Å is characteristic of a C–O single bond, and is substantially longer than found in the related homonuclear tri-iron complexes $[NEt_4][Fe_3(\mu\text{-}OCMe)(CO)_9]$[1.32(2) Å]

Table 6. Selected internuclear separations (Å) and angles (°) for $[WFe_2(\mu_3\text{-}CC_6H_4Me\text{-}4)(\mu\text{-}PPh_2)_2(CO)_6(\eta\text{-}C_5H_5)]$ (**8**) with e.s.d.s in parentheses

W–Fe(1)	2.735(1)	W–Fe(2)	2.783(1)	W–P(1)	2.363(2)	W–C(1)	2.535(9)
W–C(6)	1.987(7)	W–C(7)	2.085(6)	Fe(1)–Fe(2)	2.572(1)	Fe(1)–P(1)	2.248(2)
Fe(1)–P(2)	2.194(2)	Fe(1)–C(4)	1.808(8)	Fe(1)–C(5)	1.762(7)	Fe(1)–C(7)	1.989(6)
Fe(2)–P(2)	2.229(2)	Fe(2)–C(1)	1.791(7)	Fe(2)–C(2)	1.797(10)	Fe(2)–C(3)	1.753(10)
Fe(2)–C(7)	2.052(6)	P(1)–C(11)	1.830(9)	P(1)–C(21)	1.820(7)	P(2)–C(31)	1.840(8)
P(2)–C(41)	1.832(6)	C(1)–O(1)	1.170(9)	C(2)–O(2)	1.13(1)	C(3)–O(3)	1.16(1)
C(4)–O(4)	1.12(1)	C(5)–O(5)	1.153(8)	C(6)–O(6)	1.156(8)	C(7)–C(51)	1.459(8)
Fe(1)–W–Fe(2)	55.6(1)	Fe(1)–W–P(1)	51.7(1)	Fe(2)–W–P(1)	106.8(1)	Fe(1)–W–C(6)	84.5(2)
Fe(2)–W–C(6)	83.7(2)	P(1)–W–C(6)	82.6(2)	Fe(1)–W–C(7)	46.3(2)	Fe(2)–W–C(7)	47.2(2)
P(1)–W–C(7)	85.4(2)	C(6)–W–C(7)	122.6(3)	W–Fe(1)–Fe(2)	63.2(1)	W–Fe(1)–P(1)	55.6(1)
Fe(2)–Fe(1)–P(1)	118.2(1)	W–Fe(1)–P(2)	115.9(1)	Fe(2)–Fe(1)–P(2)	55.1(1)	P(1)–Fe(1)–P(2)	169.1(1)
C(4)–Fe(1)–C(5)	103.2(3)	W–Fe(1)–C(7)	49.3(2)	Fe(2)–Fe(1)–C(7)	51.6(2)	P(1)–Fe(1)–C(7)	90.9(2)
P(2)–Fe(1)–C(7)	78.3(2)	W–Fe(2)–Fe(1)	61.3(1)	W–Fe(2)–P(2)	112.8(1)	Fe(1)–Fe(2)–P(2)	53.8(1)
C(1)–Fe(2)–C(2)	84.8(4)	C(1)–Fe(2)–C(3)	91.6(4)	C(2)–Fe(2)–C(3)	103.7(5)	W–Fe(2)–C(7)	48.2(2)
Fe(1)–Fe(2)–C(7)	49.4(2)	P(2)–Fe(2)–C(7)	76.2(2)	W–P(1)–Fe(1)	72.7(1)	W–P(1)–C(11)	122.7(2)
Fe(1)–P(1)–C(11)	118.1(3)	W–P(1)–C(21)	121.3(2)	Fe(1)–P(1)–C(21)	118.8(2)	C(11)–P(1)–C(21)	102.5(4)
Fe(1)–P(2)–Fe(2)	71.1(1)	Fe(1)–P(2)–C(31)	119.3(3)	Fe(2)–P(2)–C(31)	120.3(2)	Fe(1)–P(2)–C(41)	124.1(2)
Fe(2)–P(2)–C(41)	124.8(2)	C(31)–P(2)–C(41)	98.3(3)	W–C(1)–O(1)	122.5(7)	Fe(2)–C(1)–O(1)	159.4(8)
Fe(2)–C(2)–O(2)	178.2(8)	Fe(2)–C(3)–O(3)	175.6(6)	Fe(1)–C(4)–O(4)	177.0(8)	Fe(1)–C(5)–O(5)	175.5(7)
W–C(6)–O(6)	176.5(6)	W–C(7)–Fe(1)	84.3(2)	W–C(7)–Fe(2)	84.5(2)	Fe(1)–C(7)–Fe(2)	79.1(2)
W–C(7)–C(51)	132.0(4)	Fe(1)–C(7)–C(51)	133.7(4)	Fe(2)–C(7)–C(51)	124.5(5)		

Table 7. Selected internuclear distances (Å) and angles (°) for $[WFe_2(\mu_3\text{-}OCCH_2C_6H_4Me\text{-}4)(\mu\text{-}PPh_2)_2(CO)_5(\eta\text{-}C_5H_5)]$ (**9**) with e.s.d.s in parentheses

W–Fe(1)	2.723(1)	W–Fe(2)	2.712(1)	W–P(1)	2.412(2)	W–C(5)	2.155(7)
W–O(5)	2.129(6)	W–C(9)	2.020(11)	Fe(1)–Fe(2)	2.616(2)	Fe(1)–P(2)	2.149(3)
Fe(1)–C(5)	1.913(10)	Fe(1)–C(3)	1.753(10)	Fe(1)–C(4)	1.793(12)	Fe(2)–P(1)	2.255(2)
Fe(2)–P(2)	2.256(2)	Fe(2)–C(1)	1.796(11)	Fe(2)–C(2)	1.780(11)	Fe(2)–O(5)	2.011(6)
P(1)–C(11)	1.838(7)	P(1)–C(21)	1.829(5)	P(2)–C(31)	1.847(6)	P(2)–C(41)	1.856(7)
C(1)–O(1)	1.13(2)	C(5)–O(5)	1.43(1)	C(5)–C(6)	1.55(1)	C(2)–O(2)	1.13(1)
C(3)–O(3)	1.16(1)	C(4)–O(4)	1.14(1)	C(6)–C(51)	1.53(1)	C(6)–H(6a)	1.16(9)
C(6)–H(6b)	1.11(8)	C(9)–O(9)	1.13(1)				
Fe(1)–W–Fe(2)	57.6(1)	Fe(1)–W–P(1)	106.8(1)	Fe(2)–W–P(1)	51.8(1)	Fe(1)–W–C(5)	44.3(3)
Fe(2)–W–C(5)	66.4(2)	P(1)–W–C(5)	112.5(2)	Fe(1)–W–O(5)	69.3(1)	Fe(2)–W–O(5)	47.2(2)
P(1)–W–O(5)	76.9(1)	C(5)–W–O(5)	39.0(3)	W–Fe(1)–Fe(2)	61.0(1)	W–Fe(1)–P(2)	112.3(1)
Fe(2)–Fe(1)–P(2)	55.5(1)	W–Fe(1)–C(5)	51.9(2)	Fe(2)–Fe(1)–C(5)	71.5(2)	P(2)–Fe(1)–C(5)	86.7(3)
C(3)–Fe(1)–C(4)	91.6(5)	W–Fe(2)–Fe(1)	61.4(1)	W–Fe(2)–P(1)	57.2(1)	Fe(1)–Fe(2)–P(1)	115.7(1)
W–Fe(2)–P(2)	109.2(1)	Fe(1)–Fe(2)–P(2)	51.7(1)	P(1)–Fe(2)–P(2)	166.4(1)	C(1)–Fe(2)–C(2)	97.6(5)
W–Fe(2)–O(5)	51.0(2)	Fe(1)–Fe(2)–O(5)	73.2(2)	P(1)–Fe(2)–O(5)	83.0(1)	P(2)–Fe(2)–O(5)	87.8(1)
W–P(1)–F(2)	70.9(1)	W–P(1)–C(11)	124.2(3)	Fe(2)–P(1)–C(11)	118.2(2)	W–P(1)–C(21)	120.5(2)
Fe(2)–P(1)–C(21)	116.7(2)	Fe(1)–P(2)–Fe(2)	72.8(1)	Fe(1)–P(2)–C(31)	122.0(2)	Fe(2)–P(2)–C(31)	117.1(2)
Fe(1)–P(2)–C(41)	125.5(2)	Fe(2)–P(2)–C(41)	117.5(2)	Fe(2)–C(1)–O(1)	177.4(8)	W–C(5)–Fe(1)	83.8(4)
W–C(5)–O(5)	69.5(3)	Fe(1)–C(5)–O(5)	112.9(6)	W–C(5)–C(6)	133.2(5)	Fe(1)–C(5)–C(6)	130.0(5)
O(5)–C(5)–C(6)	111.7(8)	Fe(2)–C(2)–O(2)	179.4(9)	Fe(1)–C(3)–C(6)	176.7(9)	Fe(1)–C(4)–O(4)	178.8(7)
W–O(5)–Fe(2)	81.8(2)	W–O(5)–C(5)	71.5(4)	Fe(2)–O(5)–C(5)	102.3(5)	C(51)–C(6)–C(5)	120.1(5)
W–C(9)–O(9)	161.9(7)						

and $[Fe_3(\mu\text{-}H)(\mu_3\text{-}OCMe)(CO)_9]$[1.325(5) Å].[7] The marked reduction of the acyl C–O bond order found in (**9**) and to a lesser extent in $[WOs_3(\mu_3\text{-}OCCH_2C_6H_4Me\text{-}4)(CO)_{11}(\eta\text{-}C_5H_5)]$[$RCH_2C$–O 1.37(2) Å] may well reflect a strong interaction between the acyl oxygen atoms and the oxophilic tungsten centres in these clusters.

Spectroscopic data were consistent with the solid-state structure of complex (**9**) being maintained in solution. The i.r. spectrum in CH_2Cl_2 showed four absorptions attributable to terminal CO ligands and a broad band at 1 785 cm^{-1} indicating the presence of a semi-bridging CO ligand. Several weak bands were observed in the region 1 550—1 450 cm^{-1} but none of these peaks could be unambiguously assigned to the expected acyl C–O stretch. The ^1H n.m.r. spectrum showed an AB quartet at δ 3.43 p.p.m. [*J*(HH) 16 Hz] which may be assigned to the diastereotopic protons of the $\mu_3\text{-}OCC\mathit{H}_2R$ fragment, and the $^{31}P\text{-}\{^1H\}$ n.m.r. spectrum confirms the presence of $\mu\text{-}PPh_2$ ligands bridging W–Fe and Fe–Fe bonds. In the $^{13}C\text{-}\{^1H\}$ n.m.r. spectrum the acyl carbon of the $\mu_3\text{-}O\mathit{C}CH_2R$ ligand gives rise to a singlet at δ 258.8 p.p.m. which is appreciably more shielded than found for the $\mu\text{-}O\mathit{C}CH_2R$ atom in (**10**) (δ 294.4 p.p.m.)

The structure of the minor acyl complex (**10**) produced in the reaction of (**1**) with excess of PPh_2H is shown in Figure 4 and selected bond length and angle data are in Table 8. The molecular structure of the 50 cluster-valence-electron complex consists of a W–Fe–Fe chain of metal atoms. The W–Fe and Fe–Fe bonds are both bridged by $\mu\text{-}PPh_2$ ligands and a terminal PPh_2H ligand is attached to the Fe(1) end of the metal chain. The W–Fe–Fe chain is bent [W–Fe(2)–Fe(1) 147.7(1)°] and comparable deviations from linearity have been observed in the related complexes $[Mn_2Pt(\mu\text{-}PPh_2)_2(CO)_9]$[Mn–Pt–Mn 159.54(6)°][8] and $[Fe_2Rh(\mu\text{-}PPh_2)_2(\mu\text{-}CO)_2(CO)_2(\eta^5\text{-}C_5H_4Me)_2][PF_6]$ [Fe–Rh–Fe 145.03(5)°].[9] The Fe–Fe bond is spanned by a μ-acyl ligand which now formally acts as a three-

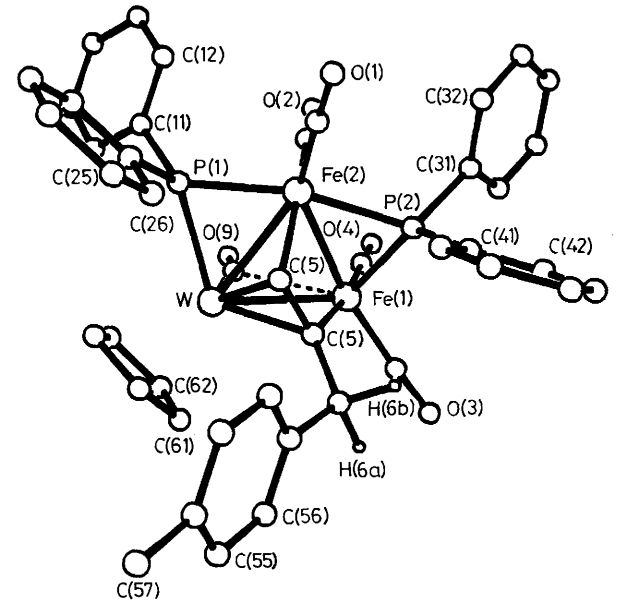

Figure 3. Molecular structure of [WFe$_2$(μ$_3$-OCCH$_2$C$_6$H$_4$Me-4)(μ-PPh$_2$)$_2$(CO)$_5$(η-C$_5$H$_5$)] (**9**) showing the atom numbering scheme

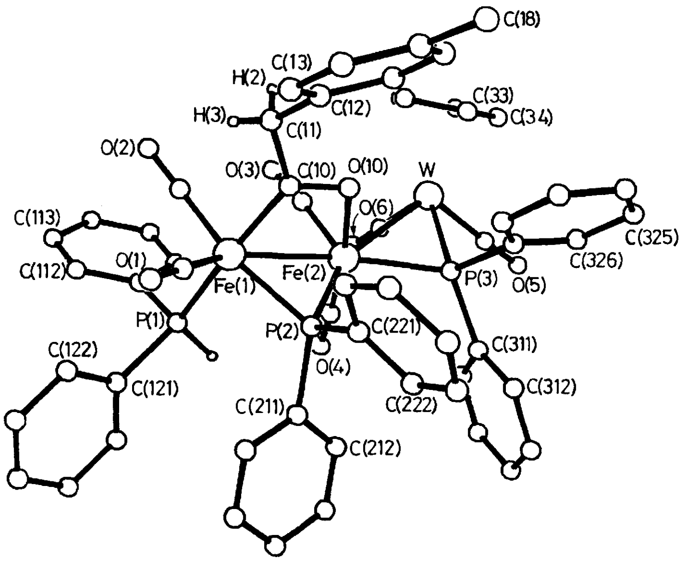

Figure 4. Molecular structure of [WFe$_2$(μ$_3$-OCCH$_2$C$_6$H$_4$Me-4)(μ-PPh$_2$)$_2$(CO)$_6$(PPh$_2$H)(η-C$_5$H$_5$)]·CH$_2$Cl$_2$ (**10**) showing the atom numbering scheme

electron donor. Bonding in μ-acyl ligands has been discussed in terms of the relative contributions of the acyl and oxyalkylidene resonance forms shown below. The μ-acyl C–O separations in (**10**) [1.255(6) Å] and in the related complexes [Fe$_2$(μ-OCMe)(μ-PPh$_2$)(CO)$_5$(PMePh$_2$)]^{10} (average 1.247 Å), [MoMn(μ-OCC$_6$H$_{11}$)(μ-PPh$_2$)(CO)$_6$(η-C$_5$H$_5$)]^{11} [1.26(1) Å], and [WRe(μ-OCCH$_2$C$_6$H$_4$Me-4)(μ-dppm)(CO)$_6${P(OMe)$_3$}]^{12} [1.248(7) Å] are appreciably shorter than the μ$_3$-acyl C–O separation in (**9**) [1.43(1) Å]. Evidently the C–O bond in (**10**) retains significant multiple-bond character, reflecting a major contribution from the acyl resonance form. The Fe(1)-C(acyl) distance of 1.936(4) Å is comparable with that observed in [Fe$_2$(μ-OCMe)(μ-PPh$_2$)(CO)$_5$(PMePh$_2$)]^{10} (average 1.957 Å). Slightly shorter Fe–C(acyl) separations are found in the complexes [MnFe(μ-OCMe)(μ-PPh$_2$)(CO)$_5$(η-C$_5$H$_5$)]^{13} (average 1.921 Å) and [MoFe(μ-OCMe)(μ-PPh$_2$)(CO)$_3$(η-C$_5$H$_5$)$_2$]^{14} [1.906(3) Å] and this is consistent with these species possessing more oxyalkylidene character than complex (**10**).

The solution i.r. spectrum of complex (**10**) showed six bands attributable to terminal carbonyl ligands. A weak absorption at 1 480 cm^{-1} may be tentatively assigned to the acyl C–O group. A similar band at 1 483 cm^{-1} in the solution i.r. spectrum of [Fe$_2$(μ-OCMe)(μ-PPh$_2$)(CO)$_5$(PMePh$_2$)] has previously been ascribed to the CO function of the μ-acetyl moiety.^{10} The ^{1}H n.m.r. spectrum showed an AB quartet at δ 4.29 p.p.m. [*J*(HH) 17 Hz] which may be assigned to the diastereotopic protons of the μ-OCC*H*$_2$R fragment and the ^{31}P-{^{1}H} n.m.r. spectrum showed the expected resonances for both the bridging and the terminal phosphine ligands. In the ^{13}C-{^{1}H} n.m.r. spectrum the μ-O*C*CH$_2$R carbon gives rise to a resonance at δ 294.4 p.p.m. [dd, *J*(PC) 25, 18 Hz] which is similar to that observed for the μ-O*C*R centres in the complexes [Fe$_2$(μ-OCMe)(μ-PPh$_2$)(CO)$_5$(PMePh$_2$)]^{10} (δ 299.6 p.p.m.) and [WRe(μ-OCCH$_2$C$_6$H$_4$Me-4)(μ-dppm)(CO)$_6${P(OMe)$_3$}]^{12} (δ 284.5 p.p.m.). More deshielded μ-O*C*R resonances are found for the complexes [MnFe(μ-OCMe)(μ-PPh$_2$)(CO)$_5$(η-C$_5$H$_5$)]^{13} (δ 319.3 p.p.m.) and [MoFe(μ-OCMe)(μ-PPh$_2$)(CO)$_3$(η-C$_5$H$_5$)$_2$]^{14} (δ 324.4 p.p.m.) and once again this is consistent with these species having more oxyalkylidene character than (**10**).

A possible mechanism by which complexes (**8**)—(**10**) are formed from (**1**) in the presence of excess of PPh$_2$H is shown in Scheme 2. Initial attack of PPh$_2$H on (**1**) affords a terminal PPh$_2$H intermediate (**A**), analogous to the moderately stable PEt$_2$H complex (**3**). At low concentrations of PPh$_2$H, (**A**) cleanly rearranges to give the μ-PPh$_2$ bridged complex (**7**) which we have established reacts with a further molecule of PPh$_2$H to give the bis(μ-PPh$_2$) complex (**8**). Since (**7**) with PPh$_2$H does not give the acyl complexes (**9**) and (**10**) these must arise from attack of a second molecule of PPh$_2$H upon (**A**) giving the bis(terminal PPh$_2$H) intermediate (**B**). Formation of (**B**) will clearly be favoured by high concentrations of PPh$_2$H. Subsequent rearrangement of (**B**) to a μ-alkyl intermediate (**E**), followed by CO insertion, could then give the μ$_3$-acyl complex (**9**). At very high concentrations of PPh$_2$H attack of a third molecule of PPh$_2$H on either (**B**) or (**E**), with concomitant ring opening, provides a route to the μ-acyl complex (**10**).

Shapley *et al.*^{15} have shown that thermolysis of the μ$_3$-acyl compound [WOs$_3$(μ$_3$-OCCH$_2$C$_6$H$_4$Me-4)(CO)$_{11}$(η-C$_5$H$_5$)] affords the oxo-alkylidyne complex [WOs$_3$(μ-O)(μ$_3$-CCH$_2$C$_6$H$_4$Me-4)(CO)$_9$(η-C$_5$H$_5$)] *via* cleavage of the acyl C–O bond. Further thermolysis of the latter oxo complex at 111 °C under N$_2$ gave [WOs$_3$(μ-H)(μ-O){μ-C=C(H)C$_6$H$_4$Me-4}(CO)$_9$(η-C$_5$H$_5$)], whilst the same reaction in the presence of H$_2$ gave the alkylidene complex [WOs$_3$(μ-H)(μ-O){μ-C(H)CH$_2$C$_6$H$_4$Me-4}(CO)$_9$(η-C$_5$H$_5$)]. It was therefore of interest to examine related reactions of (**9**) and (**10**). Thermolysis of the μ-acyl complex (**10**) in refluxing toluene (111 °C) led to the formation of the μ$_3$-acyl complex (**9**), a reaction involving loss of the terminal PPh$_2$H ligand and a CO group, with concomitant formation of a W–Fe bond. Unfortunately prolonged thermolysis of (**10**) at temperatures up to 142 °C did not lead to any evidence of acyl C–O bond cleavage, and when the reaction was repeated under H$_2$ (6 atm, *ca.* 6 × 10^5 Pa) a plethora of complexes were formed which could not be separated.

Experimental

Light petroleum refers to that fraction of b.p. 40—60 °C. All

Table 8. Selected internuclear distances (Å) and angles (°) for [$WFe_2(\mu\text{-}OCCH_2C_6H_4Me\text{-}4)(\mu\text{-}PPh_2)_2(CO)_6(PPh_2H)(\eta\text{-}C_5H_5)$] (**10**) with e.s.d.s in parentheses

W–Fe(2)	2.940(1)	W–P(3)	2.392(1)	W–C(5)	1.938(7)	W–C(6)	1.960(7)
Fe(1)–Fe(2)	2.667(1)	Fe(1)–P(1)	2.296(1)	Fe(1)–P(2)	2.213(1)	Fe(1)–C(10)	1.936(4)
Fe(1)–C(1)	1.756(6)	Fe(1)–C(2)	1.808(6)	Fe(2)–P(2)	2.232(1)	Fe(2)–P(3)	2.270(1)
Fe(2)–O(10)	2.038(3)	Fe(2)–C(4)	1.757(5)	Fe(2)–C(3)	1.823(6)	P(2)–C(111)	1.832(6)
P(1)–C(121)	1.829(5)	P(1)–H(1)	1.20(6)	P(2)–C(211)	1.835(5)	P(2)–C(221)	1.832(6)
P(3)–C(311)	1.828(5)	P(3)–C(321)	1.840(6)	C(10)–C(11)	1.512(7)	C(10)–O(10)	1.255(6)
C(11)–C(12)	1.499(8)	C(11)–H(2)	1.00(6)	C(11)–H(3)	0.80(7)	C(4)–O(4)	1.150(6)
C(1)–O(1)	1.147(8)	C(2)–O(2)	1.138(8)	C(3)–O(3)	1.149(8)	C(5)–O(5)	1.177(9)
C(6)–O(6)	1.157(8)	C–Cl(1)	1.69(2)	C–Cl(2)	1.76(2)		
Fe(2)–W–P(3)	49.1(1)	Fe(2)–W–C(5)	78.8(3)	P(3)–W–C(5)	82.6(2)	Fe(2)–W–C(6)	87.2(2)
P(3)–W–C(6)	111.3(2)	C(5)–W–C(6)	78.8(3)	Fe(2)–Fe(1)–P(1)	98.2(1)	Fe(2)–Fe(1)–P(2)	53.5(1)
P(1)–Fe(1)–P(2)	93.5(1)	Fe(2)–Fe(1)–C(10)	67.8(1)	P(1)–Fe(1)–C(10)	162.6(2)	P(2)–Fe(1)–C(10)	86.3(2)
Fe(2)–Fe(1)–C(1)	144.6(2)	P(1)–Fe(1)–C(1)	100.9(2)	P(2)–Fe(1)–C(1)	95.7(2)	C(10)–Fe(1)–C(1)	96.4(2)
Fe(2)–Fe(1)–C(2)	111.3(2)	P(1)–Fe(1)–C(2)	88.8(2)	P(2)–Fe(1)–C(2)	164.8(2)	C(10)–Fe(1)–C(2)	87.0(2)
C(1)–Fe(1)–C(2)	98.6(3)	W–Fe(2)–Fe(1)	147.7(1)	W–Fe(2)–P(2)	157.0(1)	Fe(1)–Fe(2)–P(2)	52.8(1)
W–Fe(2)–P(3)	52.8(1)	Fe(1)–Fe(2)–P(3)	152.1(1)	P(2)–Fe(2)–P(3)	104.3(1)	W–Fe(2)–O(10)	94.6(1)
Fe(1)–Fe(2)–O(10)	70.1(1)	P(2)–Fe(2)–O(10)	84.6(1)	P(3)–Fe(2)–O(10)	94.2(1)	W–Fe(2)–C(4)	90.7(2)
Fe(1)–Fe(2)–C(4)	103.2(2)	P(2)–Fe(2)–C(4)	92.3(2)	P(3)–Fe(2)–C(4)	92.5(2)	O(10)–Fe(2)–C(4)	173.1(2)
W–Fe(2)–C(3)	70.1(2)	Fe(1)–Fe(2)–C(3)	80.5(2)	P(2)–Fe(2)–C(3)	132.6(2)	P(3)–Fe(2)–C(3)	122.8(2)
O(10)–Fe(2)–C(3)	87.1(2)	C(4)–Fe(2)–C(3)	90.5(3)	Fe(1)–P(2)–Fe(2)	73.7(1)	W–P(3)–Fe(2)	78.1(1)
Fe(1)–C(10)–C(11)	126.4(4)	Fe(1)–C(10)–O(10)	117.5(3)	C(11)–C(10)–O(10)	115.6(4)	C(10)–C(11)–C(12)	118.0(5)
Fe(2)–O(10)–C(10)	104.0(3)	Fe(2)–C(4)–O(4)	177.5(5)	Fe(1)–C(1)–O(1)	178.9(5)	Fe(1)–C(2)–O(2)	176.2(6)
Fe(2)–C(3)–O(3)	173.5(5)	W–C(5)–O(5)	176.8(6)	W–C(6)–O(6)	177.3(5)	Cl(1)–C–Cl(2)	112.1(11)

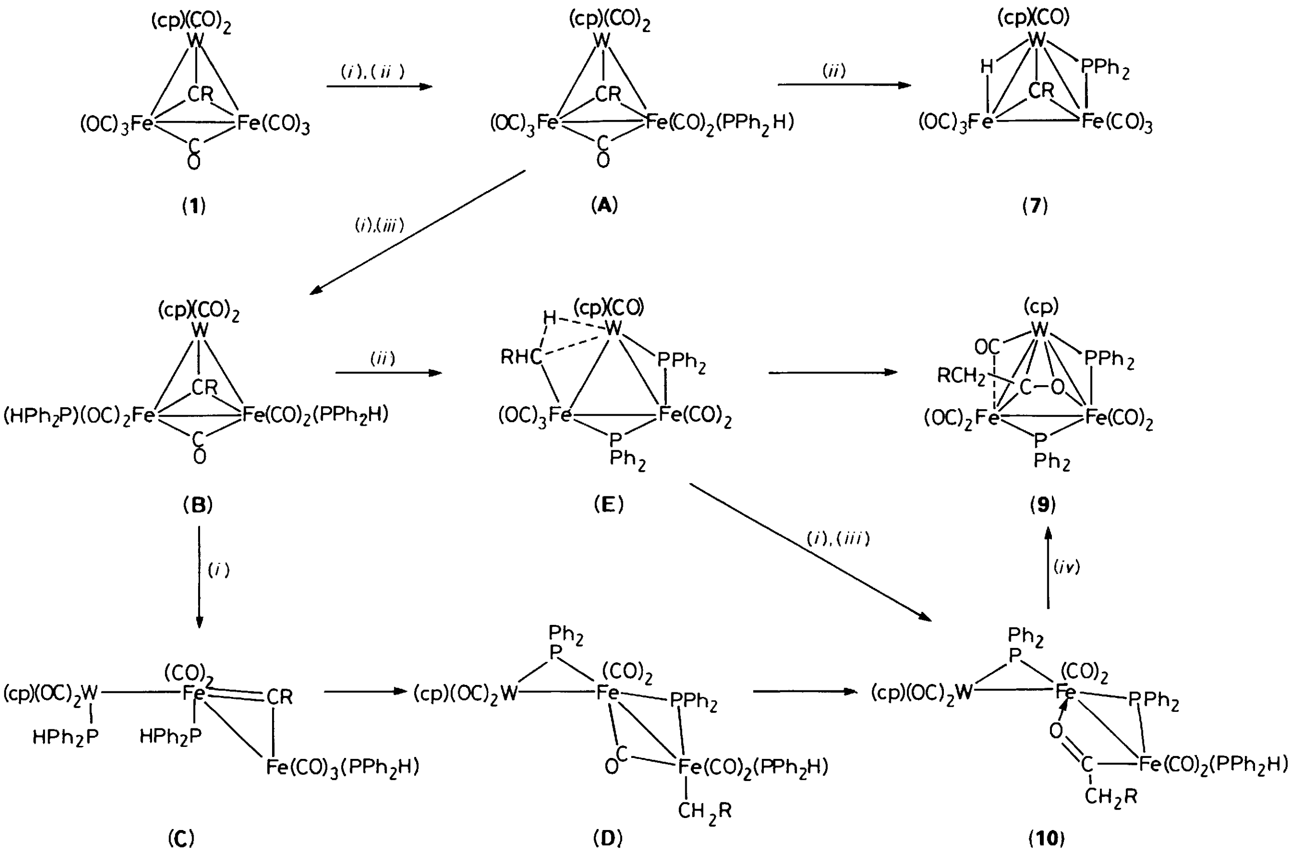

Scheme 2. R = C_6H_4Me-4. (*i*) PPh_2H; (*ii*) –CO; (*iii*) +CO; (*iv*) 111 °C, $-PPh_2H$, –CO

solvents were dried and deoxygenated before use. Experiments were carried out using Schlenk-tube techniques, under a dry oxygen-free atmosphere. The i.r. spectra were measured with Nicolet 10-MX and 5Z-DX spectrophotometers, and n.m.r spectra with JNM FX 90Q, GX 270, and GX 400 instruments. Chromatography was carried out on Aldrich Florisil (100—200 mesh) or B.D.H. alumina. The compound [$WFe_2(\mu_3\text{-}CC_6H_4Me\text{-}4)(\mu\text{-}CO)(CO)_8(\eta\text{-}C_5H_5)$] was prepared by the literature method.[4] Analytical and other data for the new compounds are listed in Tables 1—3.

Table 9. Atomic positional parameters (fractional co-ordinates × 10^4) for compound (**5**) with e.s.d.s in parentheses

Atom	x	y	z	Atom	x	y	z
W	1 746(1)	5 890(1)	8 862(1)	C(20)	1 798(7)	6 454(4)	7 773(5)
Fe(1)	255(1)	6 175(1)	7 241(1)	C(21)	2 348(7)	7 151(4)	7 691(5)
Fe(2)	2 095(1)	5 466(1)	7 256(1)	C(22)	3 474(8)	7 212(5)	7 868(7)
P(1)	2 159(2)	6 063(1)	6 053(2)	C(23)	3 953(8)	7 867(5)	7 843(8)
P(2)	2 034(2)	4 746(1)	8 422(1)	C(24)	3 358(8)	8 498(4)	7 667(5)
C(1)	−65(8)	6 673(4)	6 234(6)	C(25)	2 262(8)	8 423(4)	7 481(5)
O(1)	−345(6)	7 013(4)	5 614(4)	C(26)	1 740(7)	7 782(4)	7 488(5)
C(2)	−286(8)	6 844(5)	7 793(7)	C(27)	3 931(11)	9 212(5)	7 676(7)
O(2)	−652(6)	7 271(4)	8 127(5)	C(111)	1 163(9)	5 754(4)	5 021(5)
C(3)	−931(10)	5 605(5)	6 979(7)	C(112)	1 084(12)	6 239(6)	4 231(7)
O(3)	−1 713(7)	5 267(4)	6 789(5)	C(113)	3 480(10)	6 108(6)	5 818(8)
C(4)	1 907(8)	4 654(4)	6 662(6)	C(114)	3 856(12)	5 387(7)	5 578(10)
O(4)	1 777(7)	4 143(3)	6 244(5)	C(211)	940(8)	4 056(4)	8 191(6)
C(5)	3 533(9)	5 469(4)	7 697(6)	C(212)	816(9)	3 747(5)	9 031(7)
O(5)	4 485(6)	5 446(4)	7 978(5)	C(213)	3 296(8)	4 216(5)	8 903(6)
C(6)	287(8)	5 585(4)	8 794(6)	C(214)	3 569(9)	3 659(5)	8 342(7)
O(6)	−546(6)	5 388(4)	8 890(5)	C(50)	4 119(27)	1 863(14)	−186(19)
C(11)	2 134(12)	5 885(5)	10 383(6)	C(51)	3 259(16)	1 991(12)	137(17)
C(12)	1 863(11)	6 589(5)	10 070(6)	O(50)	3 430(11)	2 735(9)	644(9)
C(13)	2 659(12)	6 851(6)	9 715(7)	C(52)	2 879(16)	2 928(20)	1 174(14)
C(14)	3 468(10)	6 305(7)	9 820(7)	C(53)	3 216(21)	3 515(14)	1 728(25)
C(15)	3 148(12)	5 733(7)	10 220(7)				

Table 10. Atomic positional parameters (fractional co-ordinates × 10^4) for compound (**8**) with e.s.d.s in parentheses

Atom	x	y	z	Atom	x	y	z
W	2 007(1)	7 470(1)	7 996(1)	C(25)	3 283(7)	6 912(5)	10 954(4)
Fe(1)	3 721(1)	8 382(1)	8 672(1)	C(26)	3 076(6)	7 216(4)	10 240(4)
Fe(2)	3 718(1)	7 835(1)	7 379(1)	C(31)	5 774(6)	9 170(4)	8 002(4)
P(1)	2 215(1)	8 201(1)	9 081(1)	C(32)	5 832(6)	9 770(4)	8 444(5)
P(2)	5 179(1)	8 340(1)	8 236(1)	C(33)	6 345(8)	10 384(5)	8 298(7)
C(1)	2 405(7)	7 571(4)	6 716(4)	C(34)	6 765(8)	10 391(6)	7 696(7)
O(1)	1 742(5)	7 417(3)	6 133(3)	C(35)	6 732(8)	9 821(7)	7 253(6)
C(2)	3 593(7)	8 592(5)	6 762(5)	C(36)	6 230(7)	9 189(5)	7 398(5)
O(2)	3 484(6)	9 068(4)	6 369(4)	C(41)	6 498(5)	7 890(4)	8 729(4)
C(3)	4 453(7)	7 219(6)	6 995(4)	C(42)	6 841(6)	7 271(4)	8 458(4)
O(3)	4 880(6)	6 809(4)	6 700(4)	C(43)	7 872(7)	6 969(5)	8 860(5)
C(4)	3 285(6)	9 259(4)	8 305(5)	C(44)	8 552(6)	7 267(5)	9 501(5)
O(4)	3 005(5)	9 793(3)	8 046(4)	C(45)	8 226(6)	7 889(4)	9 773(5)
C(5)	4 518(6)	8 542(4)	9 633(4)	C(46)	7 200(6)	8 196(4)	9 382(4)
O(5)	5 049(5)	8 692(3)	10 248(3)	C(51)	4 471(5)	6 771(3)	8 745(4)
C(6)	1 258(6)	8 324(4)	7 436(4)	C(52)	5 195(5)	6 783(4)	9 503(4)
O(6)	772(5)	8 801(3)	7 099(3)	C(53)	5 843(6)	6 211(4)	9 832(5)
C(7)	3 749(5)	7 365(3)	8 400(3)	C(54)	5 832(7)	5 593(4)	9 429(6)
C(11)	1 289(6)	8 953(4)	9 077(4)	C(55)	5 134(7)	5 564(4)	8 683(6)
C(12)	1 725(7)	9 615(4)	9 336(6)	C(56)	4 480(6)	6 118(4)	8 355(4)
C(13)	981(10)	10 180(5)	9 265(8)	C(57)	6 558(8)	4 962(5)	9 817(8)
C(14)	−138(9)	10 091(5)	8 995(7)	C(61)	542(8)	6 790(4)	7 251(4)
C(15)	−571(7)	9 443(5)	8 750(6)	C(62)	272(6)	6 981(4)	7 911(4)
C(16)	143(6)	8 870(4)	8 802(5)	C(63)	1 050(7)	6 680(4)	8 555(5)
C(21)	2 425(5)	7 826(4)	10 034(4)	C(64)	1 805(7)	6 276(4)	8 286(6)
C(22)	1 983(7)	8 105(5)	10 577(4)	C(65)	1 490(7)	6 350(4)	7 490(5)
C(23)	2 173(8)	7 803(5)	11 290(5)	Cl	4 511(5)	706(3)	4 836(4)
C(24)	2 816(7)	7 204(5)	11 472(4)	C	4 671(23)	−95(38)	5 312(23)

Reactions.—$[WFe_2(\mu_3\text{-}CC_6H_4Me\text{-}4)(\mu\text{-}CO)(CO)_8(\eta\text{-}C_5H_5)]$ (**1**) *with* PMe_2Ph. A diethyl ether (25 cm^3) solution of complex (**1**) (0.42 g, 0.59 mmol) was treated with PMe_2Ph (0.08 g, 0.59 mmol) at 20 °C. The mixture was stirred for 3 h, after which time the i.r. spectrum indicated an absence of (**1**). The solvent was removed from the resulting orange-brown solution *in vacuo*. The residue was dissolved in the minimum volume of CH_2Cl_2–light petroleum (2:3) and chromatographed on alumina. Elution with the same solvent afforded a major orange-brown band which was collected. Removal of the solvent *in vacuo* followed by recrystallization from CH_2Cl_2–light petroleum (1:10) afforded brown *microcrystals of* $[WFe_2(\mu_3\text{-}CC_6H_4Me\text{-}4)(\mu\text{-}CO)(CO)_7(PMe_2Ph)(\eta\text{-}C_5H_5)]$ (**2**) (0.43 g).

With PEt_2H. (*i*) The complex (**1**) (0.35 g, 0.49 mmol) was dissolved in diethyl ether (30 cm^3) and PEt_2H (0.045 g, 0.50 mmol) was added. After 30 min had elapsed, the volume of the solution was reduced to *ca.* 10 cm^3 *in vacuo*, and light petroleum (20 cm^3) was added to afford brown *microcrystals of* $[WFe_2(\mu_3\text{-}CC_6H_4Me\text{-}4)(\mu\text{-}CO)(CO)_7(PEt_2H)(\eta\text{-}C_5H_5)]$ (**3**) (0.24 g).

(*ii*) A diethyl ether (30 cm^3) solution of complex (**1**) (0.27 g, 0.38 mmol) was treated with PEt_2H (0.035 g, 0.39 mmol) at

20 °C. The mixture was stirred for 3 d at this temperature, after which time the solvent was removed *in vacuo*. The residue was dissolved in CH_2Cl_2–light petroleum (3:7) and chromatographed on alumina. The major green-brown band was collected, affording a brown solution. The solvent was removed *in vacuo*. Recrystallization from CH_2Cl_2–pentane (1:10) afforded black *crystals of* $[WFe_2(\mu_3\text{-}CC_6H_4Me\text{-}4)(\mu\text{-}H)(\mu\text{-}PEt_2)(CO)_7(\eta\text{-}C_5H_5)]$ (**4**) (0.19 g).

(*iii*) A CH_2Cl_2 (10 cm^3) solution of complex (**1**) (0.6 g, 0.84 mmol) was treated with an excess of PEt_2H (0.38 g, 4.2 mmol) at 20 °C. After 12 h the solvent was removed *in vacuo*. The residue was dissolved in CH_2Cl_2–light petroleum (2:3) and chromatographed on Florisil at 7 °C. Elution with the same solvent afforded three major bands. The first green-brown band (*ca.* 15%) was identified as (**4**) by its i.r. spectrum. The second red-purple band was collected. The solvent was removed *in vacuo*, and recrystallization from CH_2Cl_2–diethyl ether–light petroleum (1:1:5) at −20 °C afforded plate-like orange-red *crystals* of $[WFe_2(\mu_3\text{-}CC_6H_4Me\text{-}4)(\mu\text{-}H)(\mu\text{-}PEt_2)(CO)_6(PEt_2H)(\eta\text{-}C_5H_5)]\cdot Et_2O$ (**5**) (0.40 g). Further elution with CH_2Cl_2–light petroleum (3:2) afforded a third orange band (*ca.* 5%). This was identified as the compound (**3**) by its i.r. spectrum.

$[WFe_2(\mu_3\text{-}CC_6H_4Me\text{-}4)(\mu\text{-}H)(\mu\text{-}PEt_2)(CO)_6(PEt_2H)(\eta\text{-}C_5H_5)]$ (**5**) (*i*) A toluene solution of complex (**5**) (0.36 g, 0.41 mmol) was refluxed at 111 °C for 4 h, after which time the solvent was removed *in vacuo*. The residue was dissolved in CH_2Cl_2–light petroleum (1:3) and chromatographed on alumina. Elution with the same solvent afforded a green-brown band which was collected. The solvent was removed *in vacuo*, and recrystallization from CH_2Cl_2–light petroleum (1:10) afforded dark brown *crystals of* $[WFe_2(\mu_3\text{-}CC_6H_4Me\text{-}4)(\mu\text{-}PEt_2)_2(CO)_6(\eta\text{-}C_5H_5)]$ (**6**) (0.23 g).

(*ii*) A thf solution of complex (**5**) (0.51 g, 0.58 mmol) was treated with $Li[BEt_3H]$ [60 μl of a 1 mol dm^{-3} solution in tetrahydrofuran (thf), 0.06 mmol] and the solution was stirred for 24 h. After this time the solvent was removed *in vacuo*. Chromatography and recrystallization as in (*i*) afforded *crystals* of (**6**) (0.29 g).

$[WFe_2(\mu_3\text{-}CC_6H_4Me\text{-}4)(\mu\text{-}CO)(CO)_8(\eta\text{-}C_5H_5)]$ (**1**) *with* PPh_2H. (*i*) A diethyl ether (25 cm^3) solution of complex (**1**) (0.42 g, 0.60 mmol) was treated with PPh_2H (0.11 g, 0.60 mmol). The mixture was stirred for 3 h, after which time the i.r. spectrum showed an absence of starting material. The solvent was removed from the resulting green solution *in vacuo*. The residue was dissolved in CH_2Cl_2–light petroleum (1:10) and chromatographed on Florisil (2 × 20 cm). Elution with the same solvent afforded an olive-green band. The solvent was removed *in vacuo* and recrystallization from CH_2Cl_2–diethyl ether–light petroleum gave dark brown crystals of $[WFe_2(\mu_3\text{-}CC_6H_4Me\text{-}4)(\mu\text{-}H)(\mu\text{-}PPh_2)(CO)_7(\eta\text{-}C_5H_5)]$ (**7**) (0.37 g).

(*ii*) A CH_2Cl_2 (1 cm^3) solution of complex (**1**) (0.62 g, 0.87 mmol) was treated with PPh_2H (0.8 g, 4.3 mmol). The mixture was stirred for 24 h, after which time the solvent was removed *in vacuo*. The residual brown oil was dissolved in the minimum volume of CH_2Cl_2–light petroleum (1:4) and chromatographed on alumina. Gradient elution with CH_2Cl_2–light petroleum (1:4 to 3:2) afforded three major bands. The first green band was identified as $[WFe_2(\mu_3\text{-}CC_6H_4Me\text{-}4)(\mu\text{-}PPh_2)_2(CO)_6(\eta\text{-}C_5H_5)]$ (**8**) (*ca.* 10%). A more efficient synthesis of compound (**8**) is described in the following section. The second brown band was collected and the solvent was removed *in vacuo*. Recrystallization from CH_2Cl_2–light petroleum (1:10) afforded dark brown *crystals* of $[WFe_2(\mu\text{-}OCCH_2C_6H_4Me\text{-}4)(\mu\text{-}PPh_2)_2(CO)_6(PPh_2H)(\eta\text{-}C_5H_5)]\cdot CH_2Cl_2$ (**10**) (0.25 g). The third grey-green band was also collected and the solvent was removed *in vacuo*. Recrystallization from CH_2Cl_2–light petroleum gave black *crystals* of $[WFe_2(\mu_3\text{-}OCCH_2C_6H_4Me\text{-}4)(\mu\text{-}PPh_2)_2(CO)_5(\eta\text{-}C_5H_5)]$ (**9**) (0.43 g).

$[WFe_2(\mu_3\text{-}CC_6H_4Me\text{-}4)(\mu\text{-}H)(\mu\text{-}PPh_2)(CO)_7(\eta\text{-}C_5H_5)]$ (**7**) *with* PPh_2H. A toluene (10 cm^3) solution of complex (**7**) (0.27 g, 0.33 mmol) was refluxed (111 °C) for 30 min to generate *in situ* a solution of the unsaturated derivative $[WFe_2(\mu_3\text{-}CC_6H_4Me\text{-}4)(\mu\text{-}H)(\mu\text{-}PPh_2)(CO)_6(\eta\text{-}C_5H_5)]$. The solvent was removed *in vacuo*, CH_2Cl_2 (10 cm^3) was added, and the resulting solution was treated with PPh_2H (0.06 g, 0.32 mmol). The solution was stirred for 24 h, after which time the solvent was removed *in vacuo*. The residue was dissolved in CH_2Cl_2–light petroleum (2:3) and chromatographed on alumina. Elution with the same solvent mixture afforded a major green band which was collected. The solvent was removed *in vacuo*, and recrystallization from CH_2Cl_2–light petroleum (1:8) afforded green *crystals* of $[WFe_2(\mu_3\text{-}CC_6H_4Me\text{-}4)(\mu\text{-}PPh_2)_2(CO)_6(\eta\text{-}C_5H_5)]\cdot 0.5CH_2Cl_2$ (**8**) (0.30 g).

Thermolysis of $[WFe_2(\mu\text{-}OCCH_2C_6H_4Me\text{-}4)(\mu\text{-}PPh_2)_2(CO)_6(PPh_2H)(\eta\text{-}C_5H_5)]$ (**10**).—A toluene (10 cm^3) solution of complex (**10**) (0.20 g, 0.15 mmol) was refluxed (111 °C) for 4 h, after which time the solvent was removed *in vacuo*. The residue was dissolved in CH_2Cl_2–light petroleum (1:1) and chromatographed on alumina. Elution with the same solvent mixture afforded a grey-green band of (**9**) (0.11 g, 73%).

Crystal Structure Determinations.—Data were collected using Nicolet $P2_1$ or $P3$ diffractometers (293 K, Mo-K_α *X*-radiation, graphite monochromator, $\bar{\lambda} = 0.710\,69$ Å). The data were corrected for Lorentz, polarization and *X*-ray absorption effects.[16] The structures were solved by conventional heavy-atom or direct methods and successive difference Fourier syntheses were used to locate all non-hydrogen atoms. Final refinements by blocked-cascade least squares were performed on a Data General 'Eclipse' computer with the SHELXTL system of programs.[16] Scattering factors with corrections for anomalous dispersion were taken from ref.17. Atom co-ordinates are given in Tables 9—12.

Additional material available from the Cambridge Crystallographic Data Centre comprises H-atom co-ordinates, thermal parameters, and remaining bond lengths and angles.

$[WFe_2(\mu_3\text{-}CC_6H_4Me\text{-}4)(\mu\text{-}H)(\mu\text{-}PEt_2)(CO)_6(PEt_2H)(\eta\text{-}C_5H_5)]\cdot Et_2O$ (**5**). Crystals of (**5**) were grown from a CH_2Cl_2–diethyl ether–light petroleum (1:1:4) solvent mixture at −20 °C as orange plates (crystal dimensions *ca.* 0.40 × 0.35 × 0.10 mm). Of the 4 238 data collected (θ—2θ scans, 2θ ⩽ 50°, weak data for 2θ ⩾ 40° were not collected), 3 660 unique data had $F \geqslant 5\sigma(F)$, and only these were used for structure solution and refinement. An empirical absorption correction was applied using a method based upon azimuthal scan data.

Crystal data. $C_{27}H_{34}Fe_2O_6P_2W\cdot Et_2O$, $M = 886.2$, monoclinic, space group $P2_1/c$, $a = 12.738(9)$, $b = 18.711(11)$, $c = 15.936(8)$ Å, $\beta = 107.69(5)°$, $U = 3\,619(4)$ Å^3, $Z = 4$, $D_c = 1.63$ g cm^{-3}, $F(000) = 1\,768$, μ(Mo-K_α) = 41.6 cm^{-1}.

The asymmetric unit contains a molecule of diethyl ether. All non-hydrogen atoms were refined with anisotropic thermal parameters. The positions of the P–H(1) and μ-H(2) hydrogen atoms were refined with fixed isotropic thermal parameters. The hydrogen atoms of the diethyl ether solvent of crystallization were not included in the refinement but all remaining non-solvent hydrogen atoms were included in calculated positions (C–H 0.96 Å) with fixed isotropic thermal parameters *ca.* $1.2U_{\text{equiv.}}$ of the parent carbon atoms. Final $R = 0.041$ ($R' = 0.044$) with a weighting scheme $w^{-1} = [\sigma^2(F) + 0.0015\,|F|^2]$. The final electron-density difference synthesis showed no peaks > 1.2 or < −0.9 e Å^{-3}.

$[WFe_2(\mu_3\text{-}CC_6H_4Me\text{-}4)(\mu\text{-}PPh_2)_2(CO)_6(\eta\text{-}C_5H_5)]\cdot 0.5CH_2Cl_2$ (**8**). Crystals of complex (**8**) were grown from CH_2Cl_2–light petroleum mixtures as black prisms [crystal dimensions *ca.* 0.255 × 0.10 × 0.075 mm with well developed faces of the

Table 11. Atomic positional parameters (fractional co-ordinates × 10^4) for compound (**9**) with e.s.d.s in parentheses

Atom	x	y	z	Atom	x	y	z
W	2 756(1)	1 795(1)	2 446(1)	C(45)	4 194	−3 613	3 719
Fe(1)	710(1)	−494(1)	3 163(1)	C(46)	3 543	−2 849	3 313
Fe(2)	2 508(1)	−453(1)	2 004(1)	C(51)	4 392(4)	604(5)	4 040(3)
P(1)	3 708(3)	1 584(2)	1 253(1)	C(52)	5 560	474	3 606
P(2)	1 216(2)	−2 219(2)	2 950(1)	C(53)	6 851	1 150	3 644
C(11)	3 169(7)	2 195(5)	427(3)	C(54)	6 975	1 956	4 116
C(12)	2 993	1 393	−44	C(55)	5 808	2 086	4 550
C(13)	2 539	1 814	−622	C(56)	4 516	1 410	4 513
C(14)	2 261	3 036	−809	C(57)	8 416(12)	2 653(10)	4 168(5)
C(15)	2 436	3 837	−337	C(61)	3 063(7)	3 011(5)	3 290(3)
C(16)	2 890	3 417	280	C(62)	2 230	3 507	2 867
C(21)	5 551(5)	1 886(6)	919(3)	C(63)	3 027	4 066	2 130
C(22)	6 245	2 514	186	C(64)	4 352	3 917	2 098
C(23)	7 648	2 710	−46	C(65)	4 374	3 265	2 815
C(24)	8 357	2 278	454	C(1)	3 552(1))	−1 349(9)	1 601(5)
C(25)	7 663	1 649	1 187	O(1)	4 171(9)	−1 957(9)	1 358(5)
C(26)	6 260	1 453	1 419	C(5)	2 494(10)	46(7)	3 315(4)
C(31)	−9(5)	−3 540(4)	2 740(3)	C(2)	1 241(10)	−700(8)	1 509(5)
C(32)	479	−4 161	2 228	O(2)	429(8)	−859(7)	1 201(4)
C(33)	−432	−5 127	2 040	C(3)	−137(11)	−921(9)	4 094(6)
C(34)	−1 830	−5 473	2 365	O(3)	−726(9)	−1 266(8)	4 709(4)
C(35)	−2 318	−4 853	2 877	C(4)	−877(10)	−740(8)	2 909(6)
C(36)	−1 408	−3 886	3 065	O(4)	−1 891(8)	−921(7)	2 755(5)
C(41)	2 119(6)	−3 209(5)	3 479(3)	O(5)	3 561(6)	158(5)	2 695(3)
C(42)	1 346	−4 334	4 050	C(6)	2 962(9)	−177(8)	4 033(4)
C(43)	1 997	−5 098	4 456	C(9)	925(10)	1 630(8)	2 215(6)
C(44)	3 421	−4 738	4 291	O(9)	65(8)	1 877(7)	1 989(5)

types (1,0,$\bar{1}$), ($\bar{1}$,0,1), (0,1,0), (0,$\bar{1}$,0), (1,0,1), ($\bar{1}$,$\bar{1}$,$\bar{1}$)]. Of the 8 069 data collected (θ–2θ scans, 2θ ⩽ 50°), 4 702 unique data had $F \geqslant 5\sigma(F)$, and only these were used for structure solution and refinement. The data were corrected for *X*-ray absorption effects by an analytical method using crystal faces.

Crystal data. $C_{43}H_{32}Fe_2O_6P_2W{\cdot}0.5CH_2Cl_2$, $M = 1\,044.6$, monoclinic, space group $P2_1/n$ (non-standard setting of $P2_1/c$), $a = 12.484(3)$, $b = 18.900(7)$, $c = 18.230(4)$ Å, $\beta = 107.48(2)°$, $U = 4\,103(2)$ Å^3, $Z = 4$, $D_c = 1.69$ g cm^{-3}, $F(000) = 2\,060$, μ(Mo-K_α) = 37.4 cm^{-1}.

All non-hydrogen atoms were refined with anisotropic thermal parameters. The asymmetric unit contains half a molecule of CH_2Cl_2 of crystallization which is disordered about the point $\frac{1}{2}$, 0, $\frac{1}{2}$. Solvent hydrogen atoms were not included in the refinement. All other hydrogen atoms were included in calculated positions (C–H 0.96 Å) with either fixed isotropic thermal parameters *ca.* $1.2U_{\text{equiv.}}$ of the parent carbon atoms (C_6H_5 and η-C_5H_5), or a common refined isotropic thermal parameter (Me-4). Final $R = 0.035$ ($R' = 0.038$) with a weighting scheme $w^{-1} = [\sigma^2(F) + 0.000\,1\,|F|^2]$. The final electron-density difference synthesis showed no peaks > 0.86 or < −0.57 e Å^{-3}.

[WFe$_2$(μ$_3$-OCCH$_2$C$_6$H$_4$Me-4)(μ-PPh$_2$)$_2$(CO)$_5$(η-C$_5$H$_5$)] (**9**). Crystals of complex (**9**) were grown from dichloromethane–light petroleum mixtures as black plates [crystal dimensions *ca.* 0.40 × 0.14 × 0.13 mm, with well developed faces of the types (1,0,0), ($\bar{1}$,0,0), (0,1,0), (0,$\bar{1}$,0), (0,0,1), (0,0,$\bar{1}$)]. Of the 7 282 data collected (θ—2θ scans, 2θ ⩽ 50°), 4 189 unique data had $F \geqslant 5\sigma(F)$, and only these were used for structure solution and refinement. The data were corrected for *X*-ray absorption effects by an analytical method using crystal faces.

Crystal data. $C_{43}H_{34}Fe_2O_6P_2W$, $M = 1\,003.6$, triclinic, space group $P\bar{1}$, $a = 10.430(7)$, $b = 10.767(9)$, $c = 19.372(20)$ Å, $\alpha = 77.37(8)$, $\beta = 78.83(7)$, $\gamma = 103.74(6)°$, $U = 1\,992(3)$ Å^3, $Z = 2$, $D_c = 1.67$ g cm^{-3}, $F(000) = 992$, μ(Mo-K_α) = 39.9 cm^{-1}.

All non-hydrogen atoms were refined with anisotropic thermal parameters. The positions of the RCH_2CO hydrogen atoms were refined with fixed isotropic thermal parameters. All remaining hydrogen atoms were included in calculated positions (C–H 0.96 Å) and chemically related groups of hydrogen atoms were given common refined isotropic thermal parameters. Final $R = 0.045$ ($R' = 0.045$) with weighting scheme $w^{-1} = [\sigma^2(F) + 0.002\,|F|^2]$. The final electron-density difference synthesis showed no peaks > 0.84 or < −1.40 Å^{-3}, except in the vicinity of the W atom where peaks of *ca.* 2.2 e Å^{-3} were observed.

[WFe$_2$(μ-OCCH$_2$C$_6$H$_4$Me-4)(μ-PPh$_2$)$_2$(CO)$_6$(PPh$_2$H)(η-C$_5$H$_5$)]·CH$_2$Cl$_2$ (**10**). Crystals of complex (**10**) were grown from dichloromethane–light petroleum mixtures as black prisms [crystal dimensions *ca.* 0.60 × 0.15 × 0.15 mm, with well developed faces of the types (1,0,0), ($\bar{1}$,0,0), (0,1,0), (0,$\bar{1}$,0), (0,0,1), (0,0,$\bar{1}$)]. Of the 7 728 data collected (θ—2θ scans, 2θ ⩽ 50°, weak data for 2θ ⩾ 40° were not collected), 7 114 unique data had $F \geqslant 5\sigma(F)$, and only these were used for structure solution and refinement. The data were corrected for *X*-ray absorption effects by an analytical method using crystal faces.

Crystal data. $C_{56}H_{45}Fe_2O_7P_3W{\cdot}CH_2Cl_2$, $M = 1\,303.4$, triclinic, space group $P\bar{1}$, $a = 11.120(4)$, $b = 13.289(4)$, $c = 19.083(5)$ Å, $\alpha = 90.96(2)$, $\beta = 99.59(2)$, $\gamma = 80.88(3)°$, $U = 2\,745(1)$ Å^3, $Z = 2$, $D_c = 1.58$ g cm^{-3}, $F(000) = 1\,300$, μ(Mo-K_α) = 28.9 cm^{-1}.

All non-hydrogen atoms were refined with anisotropic thermal parameters. The positions of the RCH_2CO and P–H hydrogen atoms were refined with fixed isotropic thermal parameters. All other hydrogen atoms were included in calculated positions (C–H 0.96 Å) with either fixed isotropic thermal parameters *ca.* $1.2U_{\text{equiv.}}$ of the parent carbon atoms (C_6H_5 and η-C_5H_5), or a common refined isotropic thermal parameter (Me-4). Final $R = 0.036$ ($R' = 0.038$) with a weighting scheme $w^{-1} = [\sigma^2(F) + 0.001\,|F|^2]$. The final electron-density difference synthesis showed no peaks > 1.14 or < −1.08 e Å^{-3}.

Table 12. Atomic positional parameters (fractional co-ordinates × 10^4) for compound (**10**) with e.s.d.s in parentheses

Atom	*x*	*y*	*z*	Atom	*x*	*y*	*z*
W	4 667(1)	2 518(1)	1 928(1)	C(214)	−2 996(7)	4 819(7)	988(4)
Fe(1)	1 708(1)	5 773(1)	2 754(1)	C(215)	−2 835(6)	5 474(6)	1 556(4)
Fe(2)	2 537(1)	3 963(1)	2 240(1)	C(216)	−1 712(5)	5 360(5)	2 019(4)
P(1)	790(1)	6 565(1)	1 696(1)	C(221)	246(4)	3 850(4)	3 303(3)
P(2)	691(1)	4 466(1)	2 555(1)	C(222)	−444(5)	3 052(4)	3 164(3)
P(3)	2 732(1)	2 237(1)	2 215(1)	C(223)	−754(6)	2 541(5)	3 724(4)
C(10)	2 833(4)	4 916(4)	3 467(3)	C(224)	−398(6)	2 813(5)	4 410(3)
C(11)	3 466(6)	5 256(4)	4 175(3)	C(225)	265(6)	3 602(5)	4 555(3)
O(10)	3 188(3)	4 012(3)	3 302(2)	C(226)	585(5)	4 124(4)	4 010(3)
C(4)	1 918(5)	4 079(4)	1 331(3)	C(311)	1 542(5)	1 684(4)	1 627(3)
O(4)	1 542(4)	4 180(3)	733(2)	C(312)	678(5)	1 210(4)	1 903(3)
C(1)	776(5)	6 401(4)	3 336(3)	C(313)	−268(6)	850(5)	1 453(4)
O(1)	175(5)	6 800(4)	3 725(3)	C(314)	−388(7)	968(5)	730(4)
C(2)	2 857(6)	6 608(4)	2 833(3)	C(315)	453(6)	1 426(5)	450(3)
O(2)	3 565(5)	7 149(4)	2 919(3)	C(316)	1 406(6)	1 772(4)	879(3)
C(3)	3 775(5)	4 651(4)	2 105(3)	C(321)	2 930(5)	1 435(4)	3 015(3)
O(3)	4 472(4)	5 166(3)	2 009(3)	C(322)	2 739(6)	1 794(5)	3 675(3)
C(5)	4 405(6)	1 409(5)	1 276(4)	C(323)	2 983(7)	1 146(5)	4 261(4)
O(5)	4 307(5)	721(4)	886(3)	C(324)	3 445(9)	130(6)	4 189(4)
C(6)	4 445(5)	3 218(5)	1 008(4)	C(325)	3 602(9)	−264(6)	3 527(4)
O(6)	4 359(5)	3 610(4)	461(3)	C(326)	3 368(7)	409(5)	2 941(4)
C(111)	1 779(5)	7 287(4)	1 294(3)	C(12)	3 506(5)	4 612(4)	4 818(3)
C(112)	1 735(6)	8 328(4)	1 384(3)	C(13)	2 917(6)	5 017(6)	5 372(4)
C(113)	2 547(6)	8 844(5)	1 122(4)	C(14)	2 906(7)	4 420(6)	5 970(4)
C(114)	3 439(7)	8 329(6)	767(4)	C(15)	3 485(6)	3 439(6)	6 036(4)
C(115)	3 500(6)	7 279(6)	675(4)	C(16)	4 098(6)	3 034(5)	5 484(3)
C(116)	2 671(6)	6 758(4)	932(3)	C(17)	4 100(6)	3 610(5)	4 885(3)
C(121)	−678(5)	7 435(4)	1 610(3)	C(18)	3 446(9)	2 754(9)	6 671(4)
C(122)	−929(6)	8 118(5)	2 139(4)	C(31)	6 534(6)	3 075(6)	2 369(4)
C(123)	−2 036(8)	8 783(6)	2 062(5)	C(32)	5 908(6)	3 107(6)	2 950(4)
C(124)	−2 890(7)	8 774(7)	1 462(5)	C(33)	5 730(6)	2 104(6)	3 089(4)
C(125)	−2 655(7)	8 103(7)	939(5)	C(34)	6 248(7)	1 462(6)	2 611(5)
C(126)	−1 547(6)	7 423(5)	1 004(4)	C(35)	6 770(6)	2 061(10)	2 168(5)
C(211)	−761(4)	4 598(4)	1 922(3)	C	8 959(14)	−867(14)	4 314(11)
C(212)	−942(6)	3 934(5)	1 357(3)	Cl(1)	7 647(6)	−56(4)	4 031(3)
C(213)	−2 066(7)	4 058(7)	898(4)	Cl(2)	10 231(6)	−529(4)	3 988(4)

Acknowledgements

We thank the S.E.R.C. for support *via* a research studentship (to J. G. L-S.).

References

1 (*a*) S. B. Colbran, B. F. G. Johnson, J. Lewis, and R. M. Sorrell, *J. Organomet. Chem.*, 1985, **296**, C1; (*b*) R. J. Haines, N. D. C. T. Steen, and R. B. English, *J. Chem. Soc., Dalton Trans.*, 1984, 515; (*c*) A. M. Arif, R. A. Jones, S. T. Schwab, and B. R. Wittlesey, *J. Am. Chem. Soc.*, 1986, **108**, 1703; (*d*) A. D. Harley, R. R. Whittle, and G. L. Geoffroy, *Organometallics*, 1986, **5**, 1283; (*e*) A. D. Horton, M. J. Mays, and P. R. Raithby, *J. Chem. Soc., Dalton Trans.*, 1987, 1557; (*f*) W. E. Buro, M. H. Chisholm, K. Folting, B. W. Eichhorn, and J. C. Huffman, *J. Chem. Soc., Chem Commun.*, 1987, 845.

2 (*a*) J. C. Jeffery and J. G. Lawrence-Smith, *J. Organomet. Chem.*, 1985, **280**, C34; (*b*) P. Dunn, J. C. Jeffery, and P. Sherwood, *ibid.*, 1986, **311**, C55; (*c*) M. R. Bradford, J. C. Jeffery, K. M. Johnson, and S. E. Phillips, *ibid.*, 1989, **362**, 205.

3 J. C. Jeffery and J. G. Lawrence-Smith, *J. Chem. Soc., Chem Commun.*, (*a*) 1985, 275; (*b*) *ibid.*, 1986, 17.

4 L. Busetto, J. C. Jeffery, R. M. Mills, F. G. A. Stone, M. J. Went, and P. Woodward, *J. Chem. Soc., Dalton Trans.*, 1983, 101.

5 G. L. Geoffroy, W. C. Mercer, R. R. Whittle, L. Markó, and S. Vastag, *Inorg. Chem.*, 1985, **24**, 3771.

6 J. T. Park, J. R. Shapley, M. R. Churchill, and C. Bueno, *Inorg. Chem.*, 1983, **22**, 1579.

7 W. K. Wong, K. W. Chiu, G. Wilkinson, A. M. R. Galas, M. B. Hursthouse, and M. Thornton-Pett, *J. Chem. Soc., Dalton Trans.*, 1983, 1557; 1981, 2496.

8 P. Braunstein, D. Matt, O. Bars, M. Louër, D. Grandjean, J. Fischer, and A. Mitschler, *J. Organomet. Chem.*, 1981, **213**, 79.

9 R. Mason and J. A. Zubieta, *J. Organomet. Chem.*, 1974, **66**, 279.

10 Y-F. Yu, J. Gallucci, and A. Wojcicki, *J. Am. Chem. Soc.*, 1983, **105**, 4826.

11 T. Adatia, K. Henrick, A. D. Horton, M. J. Mays, and M. McPartlin, *J. Chem. Soc., Chem. Commun.*, 1986, 1206.

12 J. C. Jeffery, A. G. Orpen, F. G. A. Stone, and M. J. Went, *J. Chem. Soc., Dalton Trans.*, 1986, 173.

13 R. P. Rosen, J. B. Hoke, R. R. Whittle, G. L. Geoffroy, J. P. Hutchinson, and J. A. Zubieta, *Organometallics*, 1984, **3**, 846.

14 T. S. Targos, G. L. Geoffroy, and A. L. Rheingold, *J. Organomet. Chem.*, 1986, **299**, 223.

15 J. R. Shapley, J. T. Park, M. R. Churchill, J. W. Ziller, and L. R. Beanan, *J. Am. Chem. Soc.*, 1984, **106**, 1144; M. R. Churchill, J. W. Ziller, and L. R. Beanan, *J. Organomet. Chem.*, 1985, **287**, 235; M. R. Churchill and Y-J. Li, *ibid.*, 1985, **294**, 367; 1985, **291**, 61.

16 G. M. Sheldrick, SHELXTL programs for use with a Nicolet *X*-ray System, Cambridge, 1976; updated Göttingen, 1981.

17 'International Tables for *X*-Ray Crystallography,' Kynoch Press, Birmingham, 1974, vol. 4.

Received 5th July 1989; *Paper* 9/02869B